Functional Dissociation of Paracellular Permeability and Transepithelial Electrical Resistance and Disruption of the Apical–Basolateral Intramembrane Diffusion Barrier by Expression of a Mutant Tight Junction Membrane Protein

Maria S. Balda,* J. Andrew Whitney,* Catalina Flores,‡ Sirenia González,‡ Marcelino Cereijido,‡ and Karl Matter*

*Department of Cell Biology, University of Geneva, 1211 Geneva, Switzerland; and ‡Department of Physiology, Center for Research and Advanced Studies, 07000, Mexico, D.F., Mexico

Abstract. Tight junctions, the most apical of the intercellular junctions that connect individual cells in a epithelial sheet, are thought to form a seal that restricts paracellular and intramembrane diffusion. To analyze the functioning of tight junctions, we generated stable MDCK strain 2 cell lines expressing either full-length or COOH-terminally truncated chicken occludin, the only known transmembrane component of tight junctions. Confocal immunofluorescence and immunoelectron microscopy demonstrated that mutant occludin was incorporated into tight junctions but, in contrast to full-length chicken occludin, exhibited a discontinuous junctional staining pattern and also disrupted the continuous junctional ring formed by endogenous occludin. This rearrangement of occludin was not paralleled by apparent changes in the junctional morphology as seen by thin section electron microscopy nor apparent discontinuities of the junctional strands observed by freeze-fracture. Nevertheless, expression of both wild-type and mutant occludin induced increased transepithelial electrical resistance (TER). In contrast to TER, particularly the expression of COOH-terminally truncated occludin led to a severalfold increase in paracellular flux of small molecular weight tracers. Since the selectivity for size or different types of cations was unchanged, expression of wild-type and mutant occludin appears to have activated an existing mechanism that allows selective paracellular flux in the presence of electrically sealed tight junctions. Occludin is also involved in the formation of the apical/basolateral intramembrane diffusion barrier, since expression of the COOH-terminally truncated occludin was found to render MDCK cells incapable of maintaining a fluorescent lipid in a specifically labeled cell surface domain.

INDIVIDUAL cells in a epithelial sheet are attached to each other by a set of contacts called the epithelial junctional complex (Farquhar and Palade, 1963). Tight junctions, or zonula occludens, are the most apical intercellular junction and divide the apical from the basolateral cell surface domain. Since diffusion of an extracellular high molecular weight tracer, added to an epithelial layer, is stopped at the level of the tight junctions, it is thought that tight junctions constitute a diffusion barrier (Cereijido, 1991). Thus, tight junctions allow epithelia and endothelia to separate compositionally distinct fluid phase compartments; a prerequisite for the development of most organ systems in vertebrates.

The seal provided by tight junctions does not appear to constitute an absolute diffusion barrier but to allow the passage of water and certain solutes (Cereijido et al., 1993). Studies with hydrophilic tracers in fact suggested that the paracellular pathway across epithelia involves pores with radii of 30–40 Å (Lindemann and Solomon, 1962; van Os et al., 1974). Therefore, it was proposed that selective diffusion across tight junctions is mediated by fluctuating aqueous channels embedded into tight junctional strands (Claude, 1978; Cereijido et al., 1989). If true, this model would also allow us to explain the difference between tight (low paracellular permeability and, often, high transepithelial electrical resistance (TER)[1] e.g., urinary bladder, blood-brain barrier) and leaky epithelia and endothelia (high paracellular flux and, generally, low electrical resistance, e.g., proximal renal tubule, microvessel endothelium). This classification implies, however, that TER, an instantaneous measurement for the degree of tightness, and paracellular flux, a measure for the transport capacities over a longer period of time, develop in

Address all correspondence to Dr. Karl Matter, Département de Biologie Cellulaire, Université de Genève, Sciences III, 30 Quai Earnest-Ansermet, 1211 Genève-4, Switzerland. Tel.: 41 22 702 6729. Fax: 41 22 781 1747. E-mail: Matter@Sc2A.unigue.ch

1. *Abbreviation used in this paper*: TER, transepithelial electrical resistance.

parallel. Nevertheless, if fluctuating channels within tight junctional strands exist it might be possible to modulate one parameter without significantly affecting the other.

Tight junctions also appear to be involved in the maintenance of epithelial cell polarity. Epithelial cells possess an apical cell surface, facing the organ lumen, and a basolateral domain that are separated from each other by tight junctions and that are biochemically and functionally distinct. Fluorescently labeled lipids or lipid probes cannot diffuse from one cell surface domain to the other if inserted into the outer leaflet of the plasma membrane, but can diffuse if inserted into both leaflets; hence tight junctions appear to form a fence that restricts diffusion within the outer leaflet of the plasma membrane (Dragsten et al., 1981; van Meer and Simons, 1986). Since epithelial cells are able to express at least some proteins in a polarized fashion in the absence of intercellular junctions (Vega-Salas et al., 1987), it is not clear whether this intramembrane diffusion barrier is also involved in the maintenance of protein polarity.

In freeze-fracture replicas, tight junctions appear as a netlike meshwork of fibrils formed by intramembrane particles (Staehelin, 1973). It is still not clear whether these structures are due to transmembrane proteins or specialized lipid structures. This uncertainty is due primarily to our lack of knowledge of the structural components of tight junctions and, for those we do know, their specific functions within the junctional complex. For many years, the only identified proteins of tight junctions (e.g., ZO-1, ZO-2, cingulin) were peripheral membrane proteins associated with the cytoplasmic surface of the plasma membrane and no specific function had been attributed to any of them (Anderson et al., 1993). Recently, the first transmembrane protein of tight junctions, occludin, had been identified and found to be expressed in all tested epithelia and endothelia (Furuse et al., 1993). It is not known, however, whether occludin is important for any of the specific functions of tight junctions.

We show here that stable expression of wild-type and mutant chicken occludin in MDCK cells resulted in epithelial monolayers with increased TER that allowed higher rates of paracellular flux without changing the specificity. Since the transcellular resistance of MDCK strain 2 cells is several hundred times bigger than the paracellular resistance and the total resistance cannot be bigger than either one of the two parallel resistors, this indicates that expression of occludin resulted in activation of an already existing mechanism that allows specific transport through electrically sealed tight junctions. These results directly support the idea of aqueous channels within tight junctions that might be formed or regulated by occludin. Furthermore, expression of a COOH-terminally truncated mutant occludin was found to disturb the intramembrane fence that restricts diffusion of lipids between the apical and basolateral cell surface domains. Thus, occludin is also involved in the maintenance of cell surface polarity.

Materials and Methods

Cell Culture

MDCK (strain 2) cells were grown in DMEM (4.5 g/l glucose) as described (Matter et al., 1992). For experiments, cells were plated 4–7 d before use on tissue culture–treated polycarbonate filters (Transwell; Costar Corp., Cambridge, MA) with a pore size of 0.4 μm and a diameter of 12 mm.

cDNAs, Mutagenesis, and Transfection

A cDNA coding for the NH_2-terminal half of chicken occludin was cloned by reverse transcription PCR. RNA was isolated from liver and kidney of chicken embryos and used as a template for reverse transcription using an antisense primer to the 3′-end of occludin as described for the generation of a cDNA coding for the COOH-terminal half of occludin (Fallon et al., 1995). Next, the NH_2-terminal half of occludin was amplified with a primer containing nucleotides 15–48 and an antisense primer corresponding to nucleotides 846–867 of the published occludin cDNA (Furuse et al., 1993) using Taq polymerase. PCR products were cloned into pCRII (Invitrogen Corp., San Diego, CA) and the sequences were confirmed by dideoxy sequencing. A clone with the proper sequence and the previously described cDNA coding for the COOH-terminal half of the protein was used to assemble a full length cDNA using a BglI site within the short overlap. The assembled cDNA was cloned into the EcoRI sites of Bluescript SK (for mutagenesis) and pCB6 (for transfection).

HAoccludin and HAoccludinCT3 were generated by PCR using the full-length occludin cDNA as a template. For the NH_2-terminal HA epitope a primer was used that contained a KpnI site, Kozak sequences (Kozak, 1989), the HA epitope (MQDLPGNDNSTAGL; Daro et al., 1996), and some nucleotides derived from the 5′ end of the coding sequence of occludin (5′-AAAAAGGTACCATGCAGGACCTGCCAGGCAACG-ACAACAGCACCGCCGGCCTTAAGAAGTCCTACGAVGG-3′). For HAoccludin, this primer was combined with the second primer described above and the part of the PCR product containing the relevant sequences was cloned into the wild-type sequence using KpnI and AatII. An antisense primer that converted serine-253 to a stop (5′-AAAAATCTA-GATTAGCGC GTCTTCTGGGCG-3′) was combined with the first primer mentioned above to generate HAoccludinCT3. The purified product was digested with NcoI and XbaI and the resulting fragment was used to replace the corresponding nucleotides in the cDNA coding for HAoccludin. Both constructs were verified by dideoxy sequencing.

MDCK cells were transfected, selected, and cloned as described previously (Matter et al., 1992). Cloned MDCK cells were tested for expression by immunofluorescence (see below). Homogeneously expressing clones (five for occludin, four for HAoccludin, and six, derived from two different transfections, for HAoccludinCT3) were grown up and subsequently analyzed.

Immunofluorescence

Wild-type or transfected MDCK cells were grown on glass coverslips, for screening of transfections, or on Transwell filters, for localization studies. The cells were preextracted with 0.2% Triton X-100 in 100 mM KCl, 3 mM $MgCl_2$, 1 mM $CaCl_2$, 200 mM sucrose, and 10 mM Hepes (pH 7.1) for 2 min on ice and were immediately fixed with 95% ethanol (30 min on ice). Then the samples were rehydrated with PBS. Similar results were obtained if the cells were fixed with 3% paraformaldehyde in PBS instead of ethanol. The preextraction with Triton X-100 was important for a clear labeling of ZO-1 and no staining with anti-occludin antibodies was observed if the preextraction was omitted. Nevertheless, the preextraction could be avoided if ethanol fixed samples were postfixed with acetone for 1 min. In addition to the above described fixation methods, anti-HA antibodies were also used in samples directly fixed with 3% paraformaldehyde in PBS for 20 min and subsequently permeabilized with 0.1% saponin or, alternatively, in cells fixed with methanol at −20°C for 10 min. The fixed cells were blocked for 10 min in PBS containing 0.5% BSA, 10 mM glycine, and 0.05% sodium azide (if saponin-permeabilized cells were stained, this buffer also contained 0.1% saponin). Primary antibodies were diluted in the same solution and incubated with the cells for 30–45 min. Endogenous occludin was labeled with an affinity purified polyclonal antibody (subsequently called ab A) generated against a fusion protein containing almost the entire COOH-terminal cytosolic domain that cross-reacts with rat and dog occludin (Fallon et al., 1995; see Fig. 1). Transfected chicken occludin was visualized with another antiserum (subsequently called ab B) that was raised with the same recombinant antigen but that did not cross-react with dog occludin (see Fig. 2 *A*). For the hemagglutinin epitope, a mouse monoclonal and a rabbit polyclonal antibody were used that were raised against a peptide with the sequence MQDLPGNDNSTAGL (Daro et al., 1996). Both antibodies were kindly provided by Dr. Peter van der

Sluijs (University of Utrecht) and Dr. Ira Mellman (Yale University). Rat monoclonal antibody R40.76 (kindly provided by Dr. James M. Anderson, Yale University) was used to localize ZO-1 (Anderson et al., 1988). After this first labeling step, the samples were rinsed three times with the same buffer and then incubated with affinity purified and preadsorbed secondary antibodies raised in donkeys and conjugated to DTAF or TRITC, respectively (Jackson Immunoresearch Laboratories, Inc., Westover, IA). After 30 min, the samples were washed again and mounted with Mowiol (Calbiochem Corp., La Jolla, CA). The samples were analyzed with a confocal laser scanning microscope (LSM 410 invert; Carl Zeiss, Inc., Thornwood, NY) equipped with an argon and a helium-neon laser for double fluorescence at 488 and 543 nm (emission filters: BP510-525 and LP590) using a 63× Apachromat lens.

Electron Microscopy

For the morphological analysis by thin sections, filter-grown MDCK cells were fixed with 1.0% glutaraldehyde in 100 mM sodium cacodylate buffer (pH 7.4) for 45 min. After washing, the samples were postfixed with 1% OsO_4 and subsequently processed and embedded in Epon as described (Hunziker et al., 1991). Sections were contrasted with 3% uranyl acetate and 1% lead citrate before observation.

For immunolocalization of HAoccludin and HAoccludinCT3, filter-grown MDCK cells were fixed with 3% paraformaldehyde in PBS for 30 min. Then, the cells were permeabilized and residual aldehydes were quenched by two subsequent washes of 15 min each in PBS containing 0.1% saponin, 10 mM glycine, and 0.05% sodium azide (PBS-SGS). The samples were then incubated twice for 15 min in PBS-SGS containing 1% BSA. Subsequently, the cells were labeled with the monoclonal anti-HA antibody diluted in the same buffer. After 1 h, the cells were washed three times with PBS-SGS for a total period of time of 1.5 h. After an additional incubation for 30 min in 20 mM Na_2HPO_4 (pH 8.3) containing 145 mM KCl, 0.1% saponin, and 1% BSA, the samples were labeled with protein A conjugated to colloidal gold with a diam of 5 nm (Drs. G. Posthuma and J. W. Slot, Utrecht University). After 1 h, the cells were washed six times with the same butter for a total period of time of 3 h. The samples were subsequently postfixed with 1% glutaraldehyde and embedded as described above.

For freeze fracture analysis, monolayers grown in flasks (Falcon Plastics, Cockeysvillen, MD) were fixed with 2.5% glutaraldehyde in PBS for 30 min at 37°C, washed three times with PBS, and cryoprotected by successive incubations in 10, 20, and 30% glycerol, for 30, 30, and 60 min, respectively. They were then detached from the substratum as a sheet by gently scraping with a rubber policeman, placed on gold specimen holders, and rapidly frozen in the liquid phase of partially solidified Freon 22 cooled with liquid nitrogen. Freeze fractures were performed in a Balzers BAF 400 (Balzers Company, Liechtenstein) at −150°C and 5×10^{-9} bar. Fractured faces were shadowed with platinum and carbon at 45 and 90°, respectively. Replicas were cleaned with chromic mixture and washed in distilled water, placed on 300 mesh copper grids and examined in an electron microscope (JEM-2000EX; JEOL, Tokyo, Japan).

Morphometric analysis was performed on micrographs of freeze fracture replicas, printed at a magnification of 50,000. A line parallel to the main axis of the tight junction was traced, and a series of perpendicular lines was drawn (one every 200 nm). The number of strands of a given segment of tight junctions was defined as the number of its intersections with the perpendicular line.

Protein Analysis

To detect expression by immunoblotting, filter-grown MDCK cells were washed twice with cold PBS and the filters were then cut from the frames, transferred to an eppendorf tube and boiled in SDS-PAGE sample buffer (300 μl per filter). The samples were then separated on 6–14% gradient gels and subsequently transferred to nitrocellulose. The same antibodies as described above were used to detect endogenous and transfected proteins using the ECL chemiluminescence detection system (Amersham Corp., Arlington Heights, IL).

Protein polarity was determined by cell surface biotinylation using NHS-LC-Biotin (Pierce, Rockford, IL) (Matter et al., 1993). Extraction of cells and immunoprecipitations were done as previously described (Balda et al., 1993). Na^+K^+-ATPase was immunopurified with a monoclonal antibody against the α1 chain (kindly provided by Dr. Michael Caplan, Yale University). For total proteins, the cells were extracted with PBS containing 0.5% Triton X-100. Insoluble material was removed by centrifugation and the detergent was removed from the supernatant by methanol/chloroform extraction. Biotinylation of total proteins and immunoprecipitated Na^+K^+-ATPase was determined after SDS-PAGE and transfer to nitrocellulose with HRP-conjugated streptavidin and ECL.

Transepithelial Electrical Resistance

TER was determined by applying an AC square wave current of ± 20 μA at 12.5 Hz with a silver electrode and measuring the voltage deflection elicited with a silver/silver-chloride electrode using an EVOM (World Precision Instruments) at 37°C in tissue culture medium (DME containing 10% FCS) as described (Balda et al., 1993). TER values were obtained by subtracting the contribution of the filter and bathing solution. To measure conductivity, the medium of the filter cultures was carefully aspirated and replaced by prewarmed 10 mM Hepes (pH 7.4), 1 mM sodium pyruvate, 10 mM glucose, 3 mM $CaCl_2$ containing either 145 mM NaCl (P buffer) or LiCl. The cells were incubated at 37°C for 10 min before measuring TER.

Paracellular Flux

To measure paracellular flux, FITC-dextran of various sizes was dissolved in P buffer (10 mg/ml) and dialyzed against the same buffer. A stock solution of HRP (20 mg/ml) was prepared in PBS and diluted to 10 μg/ml in P buffer before the assay. The experiment was started by transferring the filter culture to a 12-well dish containing either 500 μl per well P buffer, to measure flux in the apical to basolateral direction, or 500 μl per well of the tracer solution, to determine flux in the basolateral to apical direction. Then, 250 μl tracer solution or P buffer, respectively, was added to the apical side of the monolayers and the cells were incubated at 37°C. After 3 h, the media were collected, and FITC-dextran was measured with a fluorometer (excitation, 492 nm; emission, 520 nm), while HRP was assayed colorimetrically (Matter et al., 1994). Similar results were obtained when P buffer was replaced by tissue culture medium, and the absolute amounts of paracellular flux in wild-type and transfected cells did not depend on the direction of the concentration gradient. Paracellular flux of [^{3}H]mannitol was measured as previously using tissue culture medium (Balda et al., 1993). Removal of aliquots after 15, 30, and 60 min during the [^{3}H]mannitol experiments resulted in the same values for paracellular flux in transfected cells relative to nontransfected cells as the ones obtained after 3 h.

Fluid-phase Transcytosis

To measure fluid-phase transcytosis, cells grown on filters were allowed to take up HRP (5 mg/ml in P buffer) for 10 min at 37°C. Internalization was stopped by cooling the cells on ice. Subsequently, the cells were washed six times for 3 min with cold P buffer containing 0.5% BSA. The cultures were incubated again at 37°C for 90 min, and the media were collected and transcytosed HRP was measured with a colorimetric assay (Matter et al., 1994).

Diffusion of BODIPY-Sphingomyelin

To label cells with the fluorescent lipid, sphingomyelin/BSA complexes (5 nmol/ml) were prepared in P buffer using BODIPY-FL-sphingomyelin (Molecular Probes, Inc., Eugene, OR) and defatted BSA (Pagano and Martin, 1994). For confocal microscopy, filter-grown MDCK cells were labeled with BODIPY-sphingomyelin/BSA complexes for 10 min on ice. Then, the cells were washed with P buffer and incubated for 1 h on ice or directly prepared for microscopy. To analyze the distribution of the fluorescent lipid, the filters were cut from the frame and mounted in P buffer on a glass slide that had in each corner a drop of dried nail polish. The samples were covered with a rectangular cover slip so that it was resting on the drops of nail polish (only the two short sides were sealed with nail polish to avoid increases in pressure in the light beam). The samples were then analyzed by confocal microscopy as described above. In wild-type MDCK cells, polar lipid staining was stable for at least 20 min and lateral appearance of BODIPY-sphingomyelin was preceded by internalization. All pictures shown, however, were generated within the first 5 min of analysis.

For the fluorometric analysis, filter-grown MDCK cells were labeled as described above but for 20 min. After washing, cold 4% defatted BSA in P buffer was added to the opposite side of the monolayer. After 90 min on ice, the BSA solutions were collected and the cells were lysed in PBS containing 1% Triton X-100. Then, fluorescence extracted with BSA or deter-

gent, respectively, was quantified fluorometrically (excitation, 505; emission, 512). Approximately 80% of the fluorescence was extracted with defatted BSA if it was applied from the same side of the monolayer as the labeling. No significant amount of fluorescence was extracted if buffer without BSA was added, and there was no significant difference in total recovered fluorescence from one clone to another.

Results

Expression of Endogenous Occludin in MDCK Cells

Occludin, a membrane protein associated with tight junctions, was originally identified in chicken and was found to be expressed in various epithelial tissues (Furuse et al., 1993). This protein is also present in tight junctions of rat hepatocytes suggesting that occludin might be a common component of most, if not all, tight junctions (Fallon et al., 1995). MDCK cells grown on a permeable support are an excellent model to study the assembly and the physiological functions of tight junctions (Cereijido et al., 1978). To determine the usefulness of occludin as a tool to study the function of MDCK tight junctions, we first asked whether occludin is endogenously expressed by these cells.

Fig. 1 *A* shows a Western blot of total protein of MDCK cells incubated with a polyclonal antibody generated against a recombinant antigen containing the COOH-terminal domain of chicken occludin (ab A; Fallon et al., 1995). Similar to chicken and rat liver (Furuse et al., 1993; Fallon et al., 1995), the anti-occludin antibody recognizes a protein of ~64 kD. To test whether this immunoreactive protein is expressed in tight junctions, we processed MDCK cells grown on a permeable support for indirect double immunofluorescence using the anti-occludin antibody and monoclonal R40.76 which recognizes ZO-1, a peripheral membrane protein of tight junctions (Anderson et al., 1988). The samples were analyzed by serial confocal sections. Shown are four such confocal sections for each staining: two containing tight junctions, one derived from the area just underneath the junction, and one from near the bottom of the cells (Fig. 1 *B*). The sections show clearly that the anti-occludin antibody stains the most apical part of the lateral plasma membrane and that this region also contains ZO-1, a well-established marker for tight junctions in MDCK cells (Stevenson et al., 1989). Relative to occludin, the ZO-1 staining appears to be slightly more extended at both ends of the labeled region (e.g., *top left corners of the first panels and bottom right corners of the third panels*). It is not clear, however, whether this is due to a slightly narrower distribution of occludin or to the weaker fluorescent signal obtained with the anti-occludin antibody. Nevertheless, MDCK cells express endogenous occludin that is localized to the region of the lateral membrane corresponding to tight junctions.

Transfected Chicken Occludin and Epitope-tagged Occludin are Transported to Tight Junctions of MDCK Cells

To address questions focusing on the assembly of tight junctions and the function(s) of occludin we expressed wild-type chicken occludin and a mutant protein with an NH_2-terminal epitope derived from influenza virus hemagglutinin (Daro et al., 1996). Stably transfected MDCK cell lines were generated and analyzed by immunoblot and immunofluorescence. To distinguish between transfected and endogenous occludin, we made use of another polyclonal antibody (ab B), generated against the recombinant chicken antigen, that does not recognize dog occludin.

Immunoblots (Fig. 2 *A*) demonstrated that this anti-chicken occludin antibody (ab B) recognizes a protein of the correct molecular weight in transfected but not non-transfected (wild-type) cells indicating that it is indeed specific for chicken occludin. As expected, the anti-HA antibody recognized a specific band only in transfected MDCK cells. As shown previously for MDCK cells transfected with LDL and Fc receptor using the same expression vector (Matter et al., 1992), overnight incubation with

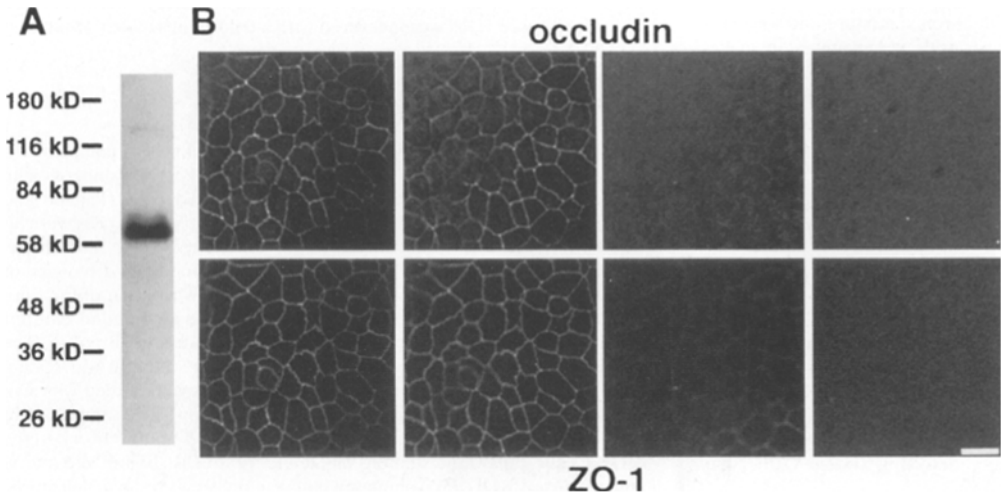

Figure 1. Expression of endogenous occludin in MDCK cells. (*A*) Filter-grown MDCK cells were lysed by boiling in SDS gel sample buffer. The sample was separated on a 6–14% gradient gel and subsequently transferred to nitrocellulose. The blot was incubated with a polyclonal antibody raised against a recombinant antigen containing the COOH-terminal domain of chicken occludin (ab A). (*B*) Filter-grown MDCK cells were fixed and processed for double immunofluorescence using the polyclonal anti-occludin antibody (ab A; *top four panels*) and monoclonal antibody R40.76 against ZO-1 (*bottom four panels*). The samples were analyzed by serial optical sections (one section every 0.9 μm). Shown, from left to right, are two subsequent sections through the junctional area, a section immediately underneath tight junctions and a section from the basal end of the cells. The background fluorescence at the base of the cells in the TRITC channel (*top right panel*) was also observed in unstained cells and appeared to be caused by reflections of the filter caused by the long wavelength laser. Bar, 10 μm.

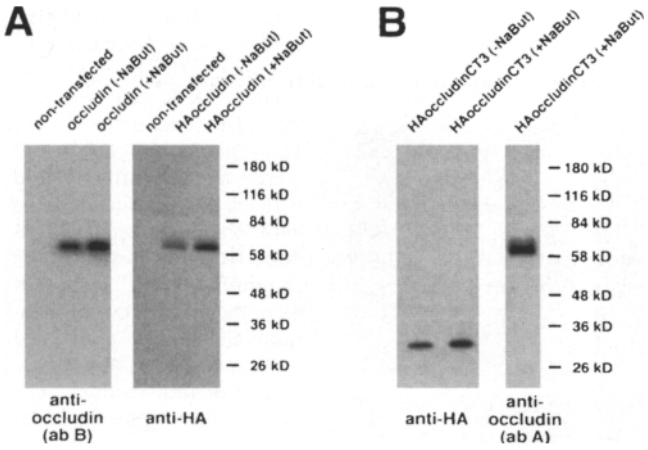

Figure 2. Expression of wild-type and mutant chicken occludin in transfected MDCK cells. Expression of chicken occludin and HAoccludin (*A*) and HAoccludinCT3 (*B*) in stably transfected MDCK cells was analyzed by immunoblots as described in Fig. 1 *A* for endogenous occludin. Chicken occludin was detected with a polyclonal antibody that did not cross-react with dog occludin in non transfected (wild-type) cells (ab B). HAoccludin and HAoccludinCT3 were visualized with a polyclonal antibody specific for the hemagglutinin epitope. Note that the anti-occludin antibody (ab A) only recognizes endogenous but not transfected occludin in cells expressing HAoccludinCT3 (*B*). In some samples, expression of the transfected cDNAs was further enhanced by an overnight incubation with 10 mM sodium butyrate.

10 mM sodium butyrate induced an increased expression of both transfected cDNAs. Thus, both proteins could be expressed in MDCK cells and detected with specific antibodies.

We next analyzed the subcellular distribution of the expressed proteins in filter-grown MDCK cells by double immunofluorescence combined with confocal microscopy. Similar to endogenous occludin, transfected chicken occludin (not shown) and HA-occludin (Fig. 3, *top sections*; shown are cells treated with sodium butyrate and stained with the anti-HA antibody) were found to colocalize with ZO-1 (*bottom sections*) in sections through the most apical part of the lateral plasma membrane. No fluorescence signal was obtained when nontransfected wild-type MDCK cells were stained with the anti-chicken occludin antibody (ab B) or the anti-HA antibody (not shown). These data suggest that chicken occludin and HAoccludin are probably integrated into tight junctions of stably transfected MDCK cells indicating that the NH_2-terminal HA epitope does not interfere with targeting and assembly.

To test whether transfected occludin is indeed incorporated into tight junctions, we labeled fixed and permeabilized cells expressing HAoccludin with the monoclonal anti-HA antibody followed by protein A-gold. After embedding in Epon, thin sections were cut and observed in an electron microscope. Fig. 4, *A–C* shows that the labeling was restricted to the region of tight junctions and was very near to the junctional membrane indicating that HAoccludin was incorporated into tight junctions of transfected MDCK cells.

Expression of Occludin Induces Increased Transepithelial Electrical Resistance

An important function of tight junctions is the formation of a tight seal between neighboring cells in an epithelial sheet. Since occludin is a membrane protein it might be involved in the sealing of tight junctions. In low resistance epithelia like MDCK strain 2, TER is a direct indicator for the tightness of the paracellular seal (González-Mariscal, 1991; Reuss, 1991). Therefore, we next measured TER of monolayers formed by wild-type and transfected cells on a permeable support. Since expression of the two occludin cDNAs did not affect the number of cells per filter (not shown), TER from different cell lines could be directly compared.

Fig. 5 *A* shows that expression of occludin and HAoccludin resulted in an increase in TER by more than a factor of two. If occludin expression was further increased by an overnight incubation with sodium butyrate (Fig. 5 *A*), the increase was approximately fourfold compared with butyrate-treated wild-type MDCK cells (Fig. 5 *B*). All tested clones expressing either chicken occludin or HAoccludin exhibited a significantly higher TER and responded with an additional increase upon induction of higher expression levels (mean values and SDs for all analyzed clones are given in the legend of Fig. 5). Different clones of cells

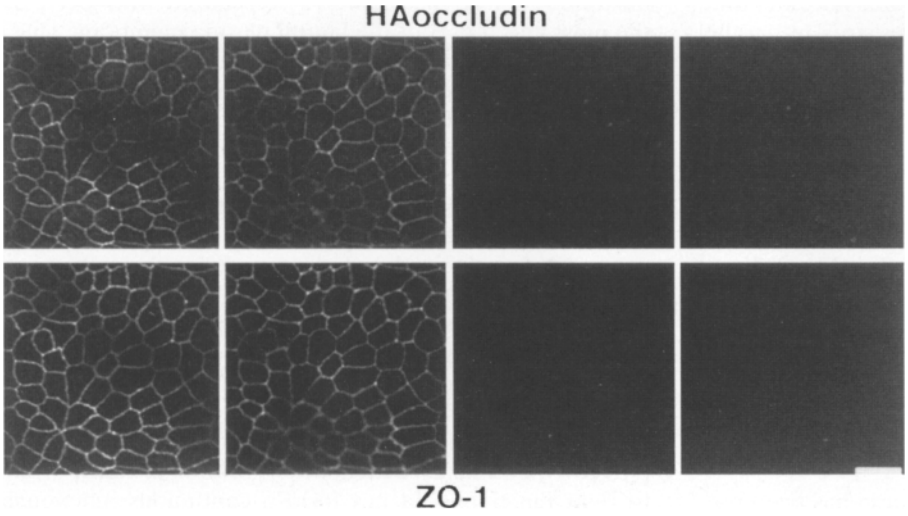

Figure 3. Subcellular distribution of HAoccludin in transfected MDCK cells. Stably transfected MDCK cells expressing HAoccludin (shown are cells induced with 10 mM sodium butyrate) were grown on filters and processed for double immunofluorescence as in Fig. 1 *B*. HAoccludin was detected with the polyclonal anti-HA antibody (*top panels*) and ZO-1 with monoclonal antibody R40.76 (*bottom panels*). Shown, from left to right, are two subsequent sections through the junctional area, a section immediately underneath tight junctions and a section from the basal end of the cells. Bar, 10 μm.

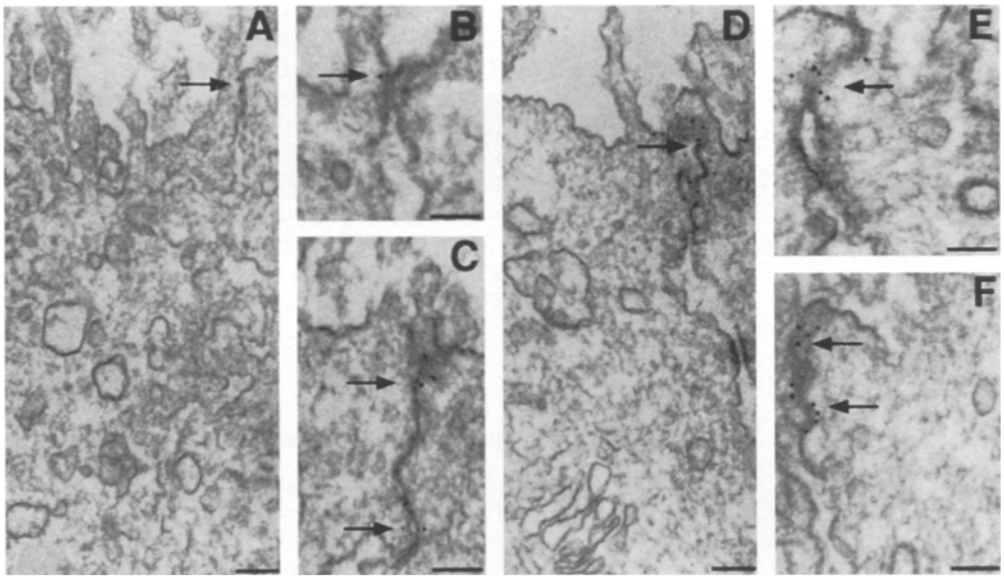

Figure 4. Transfected HAoccludin and HAoccludinCT3 are integrated into tight junctions. MDCK cells expressing HAoccludin (*A–C*) or HAoccludinCT3 (*D–F*) were fixed, permeabilized with saponin, and labeled with the monoclonal antibody anti-HA followed by protein A–gold. The cells were then postfixed with glutaraldehyde and embedded in Epon. Shown are micrographs of thin sections. The higher density of gold in labeled junctions of cells expressing HAoccludinCT3 might be caused by patches of HAoccludinCT3 observed by confocal immunofluorescence microscopy (see below). Arrows in *A* and *D* point to labeled tight junctions. *A* and *D*: Bar, 200 nm. *B*, *C*, *E*, and *F*: Bar, 150 nm.

transfected with cDNAs coding for LDL receptor using the same expression vector did not exhibit any significant change in TER (control in Fig. 5). Also clones of MDCK strain 2 cells expressing other cDNAs of proteins unrelated to tight junctions (e.g., Fc receptor, ERGIC53) generated in our laboratory never exhibited significant variations in TER (not shown). This excludes the possibility that the large increases in TER found for cells expressing chicken occludin or HAoccludin are due to clonal variations. Thus, overexpression of occludin enhances the electrical tightness of MDCK monolayers.

The total resistance of an epithelial monolayer is a function of the transcellular resistance (the sum of the resistances of the apical and basolateral plasma membrane) and the paracellular resistance (Reuss, 1991). Since these two resistors are arranged in parallel and the transcellular resistance is several hundred times bigger than the paracellular resistance in MDCK cells (González-Mariscal et al., 1989), TER essentially equals paracellular resistance in this cell line (65 to 75 Ωcm^2). Furthermore, since the total resistance of a circuit containing two resistors in parallel cannot be bigger than either one of the two single resistors, the two to fourfold increase in TER in cells expressing full-length chicken occludin must be due to a higher resistance of the paracellular pathway. This conclusion is also supported by the finding that both chicken occludin and HAoccludin were found in tight junctions (Fig. 3 and Fig. 4, *A–C*) and that the increase in TER was found to depend on the amount of expressed occludin (Fig. 2 *A* and Fig. 5).

Deletion of the COOH-terminal Domain of Occludin Causes a Discontinuous Junctional Distribution of Transfected and Endogenous Occludin

Based on its amino acid sequence, occludin has been predicted to possess four transmembrane domains with both ends in the cytosol (Furuse et al., 1993). This model was supported by the finding that the COOH-terminus of occludin can bind the cytosolic protein ZO-1 in vitro (Furuse et al., 1994). To test whether this large cytosolic COOH-terminal domain is important for the normal functioning of occludin and whether this would allow us to dissect the different functions of tight junctions, we generated MDCK cell lines expressing an epitope-tagged truncated protein lacking the entire COOH-terminal domain except the first three amino acids predicted to follow the last transmembrane domain (HAoccludinCT3). Immunoblotting with the anti-HA antibody demonstrated that this truncated protein was expressed (Fig. 2 *B*). The distribution of the mutant occludin was analyzed in monolayers grown on permeable supports by double immunofluorescence using the monoclonal anti-HA antibody, to visualize HAoccludinCT3, and another antibody specific for ZO-1.

Z-sections generated with a confocal microscope demonstrated that HAoccludinCT3 colocalized with ZO-1 in the most apical part of the lateral plasma membrane (Fig. 6 *A*) suggesting that the COOH-terminally truncated occludin was targeted to tight junctions. To confirm this, cells expressing HAoccludinCT3 were processed for immunoelectron microscopy as described above. Fig. 4, *D–F* shows that HAoccludinCT3 was indeed incorporated into tight junctions of transfected MDCK cells. Thus, the COOH-terminal cytoplasmic domain is not required for targeting of transfected occludin to tight junctions. It is not clear yet whether this means that the COOH-terminal domain does not contain any targeting information or whether the transfected mutant occludin is dragged to tight junctions due to interactions with endogenous junctional components (see below).

Horizontal sections through the same fluorescent samples revealed that HAoccludinCT3, although transported to tight junctions, did not form a continuous junctional

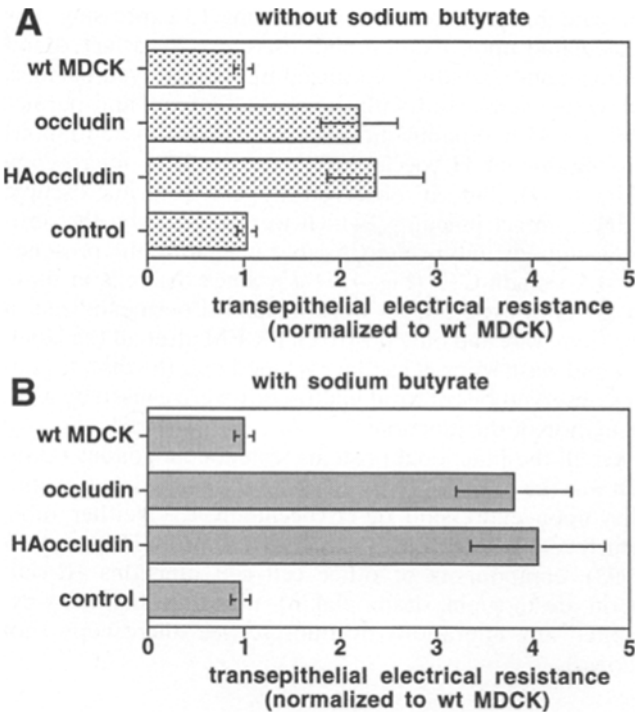

Figure 5. TER of monolayers formed by MDCK cells expressing chicken occludin and HAoccludin. Wild-type MDCK cells (*wt MDCK*) and cells expressing either chicken occludin, HAoccludin, or LDL receptor (*control*) were plated on filters for at least 4 d. TER was then measured without (*A*) or with (*B*) an overnight incubation with sodium butyrate. The background resistance obtained from empty filters was then deducted and the values were divided by the average resistance of wild-type MDCK cells. Values given represent mean values (± 1 SD) of five independent clones for occludin, four for HAoccludin, and three for control transfections. The average TER of wild-type MDCK cells was 69 ± 7 Ωcm^2 without sodium butyrate and 75 ± 9 Ωcm^2 with sodium butyrate. The values (± 1 SD) for TER (in Ωcm^2) of single clones derived from at least two independent determinations performed in duplicate were as following (the first value represents TER without and the second value, in parenthesis, with sodium butyrate): Occludin, 129 ± 19 (302 ± 34), 159 ± 15 (295 ± 24), 145 ± 22 (264 ± 33), 193 ± 12 (352 ± 20), and 120 ± 11 (215 ± 9), average of all clones 149 ± 29 (286 ± 51); HAoccludin, 170 ± 24 (316 ±16), 151 ± 10 (276 ± 28), 124 ± 10 (249 ± 17), and 210 ± 15 (375 ± 27), average of all clones 164 ± 36 (304 ± 55); control transfections, 64 ± 8 (65 ± 9), 74 ± 7 (72 ± 3), and 74 ± 6 (81 ± 8), average of all clones 71 ± 6 (70 ± 5). The TER values of monolayers formed by clones expressing occludin or HAoccludin, respectively, were significantly ($P < 0.001$ in *t* tests) higher than those of wild-type cells or control transfections.

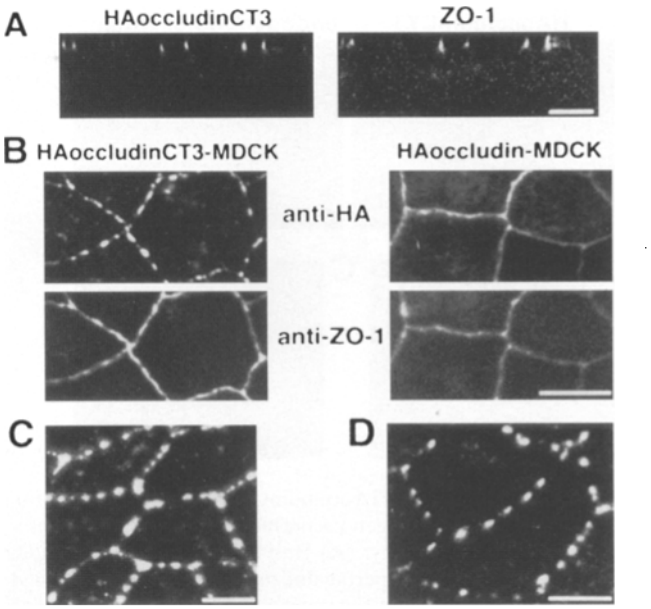

Figure 6. Subcellular distribution of HAoccludinCT3. (*A*) Filter-grown MDCK cells stably expressing HAoccludinCT3 (induced with sodium butyrate) were preextracted with Triton X-100, and fixed and processed for double immunofluorescence using the polyclonal antibody anti-HA and a monoclonal antibody recognizing ZO-1. The samples were analyzed by z-sectioning. (*B*) HAoccludinCT3- and HAoccludin-expressing cells (not preincubated with sodium butyrate), were processed and stained in the same way as the cells in *A* but analyzed by horizontal sectioning. (*C*) An extended focus of depth (four serial sections) of butyrate-treated, HAoccludinCT3-expressing cells suggests that the discontinuities were not caused by the optical sectioning. To make sure that no continuities would be missed, the photomultiplier sensitivity was increased, causing the brighter appearance of the patches). (*D*) Butyrate-treated, HAoccludinCT3-expressing cells fixed with paraformaldehyde, permeabilized with saponin, and stained with the monoclonal anti-HA antibody also exhibited a discontinuous distribution of the transfected truncated protein. Bars, 5 μm.

ring (Fig. 6 *B*). The staining of HAoccludin never revealed such discontinuities (Fig. 6 *B*). ZO-1, however, was still forming a continuous junctional pattern, similar to cells expressing HAoccludin, but appeared sometimes to be slightly more concentrated in areas that also contained HAoccludinCT3 (Fig. 6 *B*). The discontinuous distribution of HAoccludinCT3 was found not to be due to the optical sections since an extended focus of depth generated by overlaying four serial sections through the junctional area revealed the same discontinuities (Fig. 6 *C*). Additionally, the anti-HA antibody also revealed a faint intracellular staining that appeared to at least partially colocalize with a membrane protein of the Golgi complex (not shown). The same discontinuous distribution of HAoccludinCT3 was observed if the cells were directly fixed with paraformaldehyde and permeabilized with saponin (Fig. 6 *D*). Also cells fixed with ethanol/acetone or methanol (see Materials and Methods for details of the fixation methods) revealed the discontinuous distribution of HAoccludinCT3. Since all these different fixation methods resulted in the same distribution of HAoccludinCT3, it is unlikely that the discontinuities were due to a fixation artifact.

Furthermore, the staining for HAoccludinCT3 was discontinuous whether or not the cells were treated with butyrate (Fig. 6 *B* shows cells not treated with butyrate while the cells shown in *D* and *E* had been preincubated with butyrate). These immunocytochemical studies indicate that the COOH-terminal cytoplasmic domain of transfected occludin appears to be dispensable for targeting but required for the proper arrangement within tight junctions.

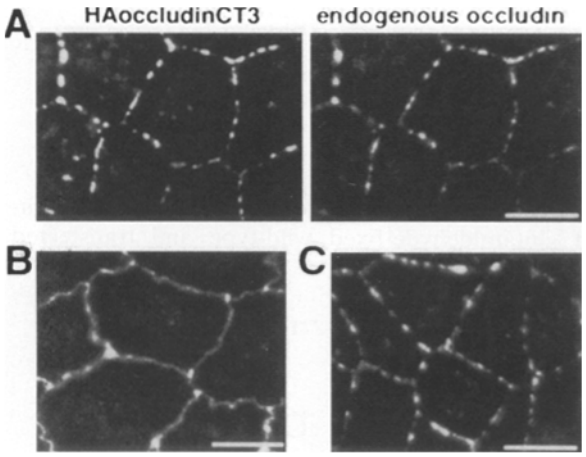

Figure 7. Transfection of HAoccludinCT3 disrupts the continuous junctional ring of endogenous occludin as observed by confocal fluorescence microscopy. (*A*) Butyrate-treated, HAoccludin CT3-expressing cells were permeabilized and fixed as in Fig. 6 *A* and subsequently stained for the transfected mutant occludin using the monoclonal anti-HA antibody and for endogenous occludin with the polyclonal anti-occludin antibody (ab A). (*B*) Butyrate-treated, wild-type MDCK, fixed and stained for endogenous occludin as in *A*, did not reveal discontinuities in the distribution of occludin. (*C*) An extended focus of depth derived from four serial sections taken from the sample as the one shown in *A* (shown is the staining for endogenous occludin) demonstrates that the discontinuities in the distribution of endogenous occludin are not due to the optical sections. Bars, 5 μm.

We next tested whether expression of HAoccludinCT3 interferes with the distribution of endogenous occludin. Since the anti-occludin antibody mentioned above (ab A) was raised against a recombinant antigen containing only the COOH-terminal cytoplasmic domain of occludin and, consequently, failed to recognize HAoccludinCT3 on immunoblots (Fig. 2 *B*), we could visualize the endogenous protein with this antibody and HAoccludinCT3 with an antibody specific for the hemagglutinin epitope.

Horizontal optical sections showed that endogenous occludin did not form a continuous junctional ring in cells expressing HAoccludinCT3 but colocalized with the truncated protein (Fig. 7 *A*). In contrast, such discontinuities were not observed in wild-type MDCK cells (Fig. 7 *B*). As above, an extended focus of depth confirmed the discontinuities (Fig. 7 *C*). Transfected cells did not exhibit lower levels of endogenous occludin by immunoblot (not shown) indicating that the gaps are not due to less protein but to a redistribution of endogenous occludin. Hence, HAoccludinCT3 not only failed to form a continuous junctional ring but also disrupted the normal distribution of endogenous occludin. This indicates that endogenous and transfected occludin appear to interact with each other. It is not clear yet whether this occurs directly or indirectly via another protein.

The finding that even endogenous occludin is discontinuously distributed in cells expressing HAoccludinCT3 also argues against the possibility that the patching could have been induced by fixation since it is difficult to imagine why the fixation properties of the same protein should be so different in different cell lines. Nevertheless, one could imagine that junctions of HAoccludinCT3-expressing cells vesiculated upon fixation and, therefore, transfected and endogenous occludin colocalized in the observed patches. However, cells fixed with paraformaldehyde and permeabilized with saponin did also exhibit the discontinuous distribution of HAoccludinCT3 by confocal microscopy (Fig. 6 *D*), but, if observed by electron microscopy, showed intact junctions, which were labeled by the anti-HA antibody and protein A–gold indicating the presence of HAoccludinCT3 (Fig. 4, *D–F*). Since the cells in these two sets of experiments were fixed and permeabilized in the same way and only postfixed for EM after all the labeling and wash steps, it can be excluded that the discontinuities observed by confocal microscopy were caused by a vesiculation of the junctions.

Of all the junctional proteins tested, endogenous occludin was the only one that significantly changed its distribution upon expression of HAoccludinCT3. Neither rab8, which colocalizes with ZO-1 in MDCK cells (Huber et al., 1993), components of other cell–cell junctions (E-cadherin, desmoglein, desmoplakin), nor actin filaments exhibited any alterations by fluorescence microscopy (not shown).

Discontinuous Distribution of Occludin in Transfected Cells Is Affected by Neighboring Wild-type Cells

Since occludin is a transmembrane component of a cell–cell junction it might interact with junctional proteins of neighboring cells. If this were true, the distribution of occludin in one cell might affect the distribution of occludin in a neighboring cell. To test this, we plated a mix of wild-type MDCK and HAoccludinCT3 transfected cells on filters. After formation of monolayers, the cells were processed for immunofluorescence and stained for HAoccludinCT3 and endogenous occludin.

Fig. 8 shows the two stainings in an optical section through the junctional area of a monolayer formed by transfected (recognizable by the weak intracellular fluorescence) and wild-type cells. If two HAoccludinCT3-expressing cells touched each other and formed junctions, endogenous occludin and transfected occludin exhibited a discontinuous staining pattern. In contrast, junctions formed by a transfected and a wild-type cell revealed only a very faint but apparently continuous staining for HAoccludinCT3. Since it could be that occludin is mediating homotypic cell–cell contacts, the uneven distribution of HAoccludinCT3 could be caused by the species difference. This is rather unlikely, however, since the intensity of the staining of HAoccludinCT3 along heterologous junctions did not change if the wild-type cells were replaced by cells expressing wild-type chicken occludin (not shown).

In the case of endogenous occludin, the discontinuities in the staining disappeared in junctions formed by a transfected and a wild-type cell. The continuous staining appeared to be brighter between cells of different origins (*arrows*) than between two wild-type cells (*arrowheads*). Transfected cells, however, did not reveal a higher level of endogenous occludin by immunoblot (not shown), and the protein did not appear to be depleted from contacts formed by the same transfected cell with another trans-

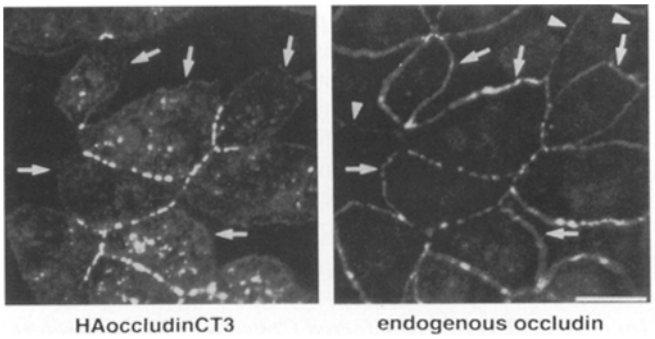

Figure 8. Neighboring wild-type cells influence the distribution of occludin in cells expressing HAoccludinCT3. Wild-type and HAoccludinCT3-expressing MDCK cells were mixed in a 1:1 ratio and plated on filters. After 4 d the cells were fixed and the distribution of endogenous occludin and HAoccludinCT3 was analyzed by double immunofluorescence as in Fig. 7 *A*. Shown are the stainings obtained in a confocal section at the level of tight junctions. Transfected cells can be recognized by the faint intracellular dots. Arrows mark borders between a transfected and a wild-type cell; arrowheads point to junctions between two wild-type cells. Bar, 5 μm.

fected cell arguing against a preferential accumulation of endogenous occludin at heterologous junctions. Since our antibody was raised against the COOH-terminal cytoplasmic domain of occludin, which is known to interact with ZO-1 (Furuse et al., 1994), it could be that the enhanced labeling was due to a better accessibility of the epitope(s) in transfected cells. This possibility is supported by the finding that in wild-type cells the antibody labels tight junctions only if the cells were extracted with Triton X-100 before fixation indicating that the detergent removes cellular components that limit the accessibility of the antibody to the COOH-terminal cytosolic domain (not shown). Nevertheless, the observation that the distribution of endogenous and transfected occludin in cells expressing HAoccludinCT3 is affected by neighboring cells expressing only full-length occludin indicates that occludin is at the very least a subunit of a complex that forms cell–cell contacts.

Expression of Full-Length and Truncated Occludin Does Not Affect the Appearance of Tight Junctions in Thin Sections

To test whether the expression of wild-type or mutant occludin affects the morphology of tight junctions, we embedded glutaraldehyde-fixed wild-type and transfected cells that had or had not been treated with butyrate in Epon. Micrographs taken from thin sections derived from some of these samples are shown in Fig. 9.

A comparison of wild-type MDCK cells that had not been (*A–C*) or had been treated with butyrate (*D–F*) did not reveal any evident morphological difference. Furthermore, the expression of chicken occludin in MDCK cells did also not cause an altered morphology of tight junctions (*G–I*, shown are butyrate-treated cells). Particularly, we did not observe an induction of multilamellar structures as it has been described for overexpression of chicken occludin in insect cells (Furuse et al., 1996). Interestingly, cells expressing HAoccludinCT3, which causes a disruption of the continuous junctional distribution of endogenous occludin, exhibited an unchanged morphology of tight junctions (*K–M*, shown are butyrate-treated cells). Thus, neither the expression of chicken occludin nor of truncated occludin affects the morphological appearance of tight junctions in MDCK cells in thin sections.

Expression of HAoccludinCT3 Results in Monolayers with Increased TER

Since we observed a discontinuous distribution of transfected and endogenous occludin in cells expressing HAoccludin CT3, it was of a particular interest to determine whether these cells would still form an electrically tight epithelial monolayer. To do this, we plated wild-type and transfected cells on filters and measured TER.

Fig. 10 *A* shows that in the absence of sodium butyrate HAoccludinCT3-transfected cells showed an increase in

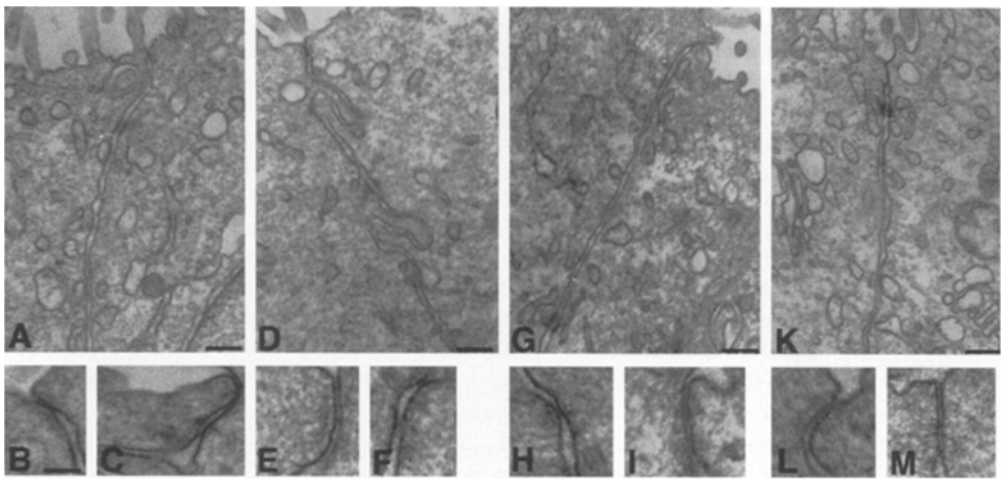

Figure 9. Transfection of wild-type and mutant occludin does not cause morphological alterations. Filter-grown wild-type and transfected MDCK cells were fixed, embedded in Epon, and thin sections were observed in an electron microscope. Shown are pictures derived from wild-type MDCK without (*A–C*) and with a preincubation with sodium butyrate (*D–F*), butyrate-treated cells expressing chicken occludin (*G–I*) or HAoccludinCT3 (*K–M*). Note that punctate apparent fusions of outer leaflets were generally not visible but that in those cases where the two adjacent membranes could be clearly resolved, the gap was filled with material with a similar density as the cytosol of the cells (e.g., *C*, *E*, *I*, *M*). Bars, 250 nm (*A*, *D*, *G*, and *K*), and 90 nm (*B*, *C*, *E*, *F*, *H*, *I*, *L*, and *M*).

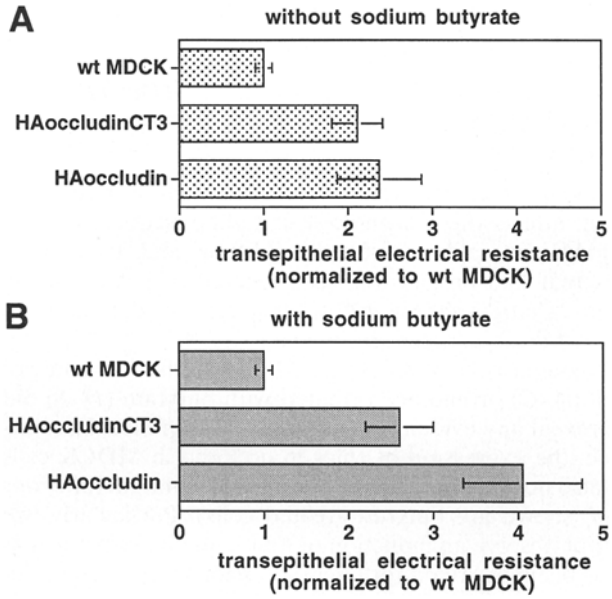

Figure 10. TER of monolayers formed by MDCK cells expressing HAoccludinCT3. Wild-type (*wt MDCK*) and transfected cells were plated and TER was measured either without (*A*) or with (*B*) an overnight incubation with sodium butyrate and calculated as described in Fig. 5. Values given represent mean values (± 1 SD) of six independent clones expressing HAoccludinCT3. The values for wild-type MDCK and HAoccludin-expressing cells are the same as the ones shown in Fig. 5 and are given to facilitate comparison (TER of these cell lines was measured at the same time). The values (± 1 SD) for TER, derived from at least two independent determinations performed in duplicate, of single clones expressing HAoccludinCT3 were as following (the first value represents TER (in Ωcm^2) without and the second value, in parenthesis, with sodium butyrate): 156 ± 18 (138 ± 20), 145 ±14 (195 ± 23), 136 ± 8 (145 ± 12), 172 ± 19 (230 ± 26), 122 ± 6 (188 ± 27), and 143 ± 10 (218 ± 15), average of all clones 146 ±17 (186 ± 37). All of these values are significantly ($P < 0.001$ in *t* tests) higher than those of wild-type cells or control transfections. TER readings of wild-type cells and cultures expressing HAoccludin or HAoccludinCT3, respectively, did not reveal fluctuations if measured over a time period of 3 h.

TER (by about a factor of 2) similar to cells expressing HAoccludin. In contrast to the latter cells, however, overnight incubation with sodium butyrate resulted in only a small additional stimulation of TER (Fig. 10 *B*) even though the induction resulted in similar levels of expression in both types of clones (Fig. 2). Nevertheless, HAoccludinCT3-expressing cells were found to be capable of establishing monolayers that were electrically tighter than those formed by wild-type MDCK cells. As in the cases of chicken occludin and HAoccludin, all tested clones, a total of six derived from two independent transfections, exhibited a significant increase in TER (mean values and SD are given in the legend of Fig. 10). As explained above, such large increases in TER of MDCK strain 2 cells must be due to changes in the paracellular resistance. Thus, also expression of COOH-terminally truncated occludin results in increased resistance of the paracellular pathway. Since transfected and endogenous occludin exhibited a discontinuous distribution if observed by fluorescence microscopy, a continuous junctional distribution of occludin does not appear to be required for the formation of electrically tight epithelial monolayers.

Increased TER in Transfected Cells Does Not Correlate with Increased Number of Strands in Freeze-Fractures

In freeze-fracture replicas, tight junctions appear as a net-like meshwork of strands formed by intramembrane particles (Staehelin, 1973). Since tissues with a high TER generally possess a higher number of those junctional strands, it has been proposed that they represent the actual diffusion barriers (Claude, 1978). Nevertheless, tight junctions with a very similar pattern of intramembrane fibrils can have very different permeabilities and electrical properties (Martínez-Palomo and Erlij, 1975, Stevenson et al., 1988, González-Mariscal et al., 1989). Since occludin appears to be closely associated with these intramembrane fibrils in tight junctions of chicken liver (Furuse et al., 1996), we tested whether expression of wild-type and mutant chicken occludin in MDCK cells causes changes in the appearance of those intramembrane fibrils.

Fig. 11 shows that the butyrate treatment by itself did not cause any major changes in the pattern of the intramembrane fibrils of control transfections (*A* without and *B* with butyrate). Identical results were obtained with wild-type MDCK cells (not shown). Furthermore, quantification of the number of strands revealed a very similar distribution under these conditions and a slight shift towards fewer number of strands in cells treated with butyrate (Fig. 12; average number of strands in untreated wild-type cells was 3.3 ± 1.6 and 2.7 ± 1.1 in butyrate-treated cells, the values for control transfections were 3.5 ± 1.9 and 2.8 ± 1.2, respectively). While it cannot be ruled out that this slight reduction is due to experimental variation, it was not paralleled by significant changes in TER (see legend of Fig. 5) or paracellular flux (see below).

We next analyzed freeze-fractures of MDCK cells expressing either chicken occludin (Fig. 11, *C* and *D*) or HAoccludin (Fig. 11, *E* and *F*). Clones with average increases in TER were chosen for the analysis (occludin: 129 ± 24 Ωcm^2 without and 302 ± 34 Ωcm^2 with butyrate; HAoccludin: 170 ± 24 Ωcm^2 without and 316 ±16 Ωcm^2). While single pictures taken from those freeze-fractures did not exhibit dramatic differences, the quantification shown in Fig. 12, which is derived from at least nine images for each clone indicated an increase in the average number of strands for cells expressing chicken occludin (3.8 ± 1.9 without and 4.7 ± 2.6 with butyrate) while no significant

Figure 11. Freeze-fracture EM of MDCK tight junctions. MDCK cells were fixed with glutaraldehyde and processed for freeze-fracture. Shown are images of replicas derived from control transfections (*A* without and *B* with sodium butyrate) and MDCK cells expressing chicken occludin (*C* without and *D* with sodium butyrate), HAoccludin (*E* without and *F* with sodium butyrate), or HAoccludinCT3 (*G* without and *H* with sodium butyrate). There were no apparent differences between the samples in the ratio of strands that fractionated with the P or the E face, respectively. Bar, 200 nm.

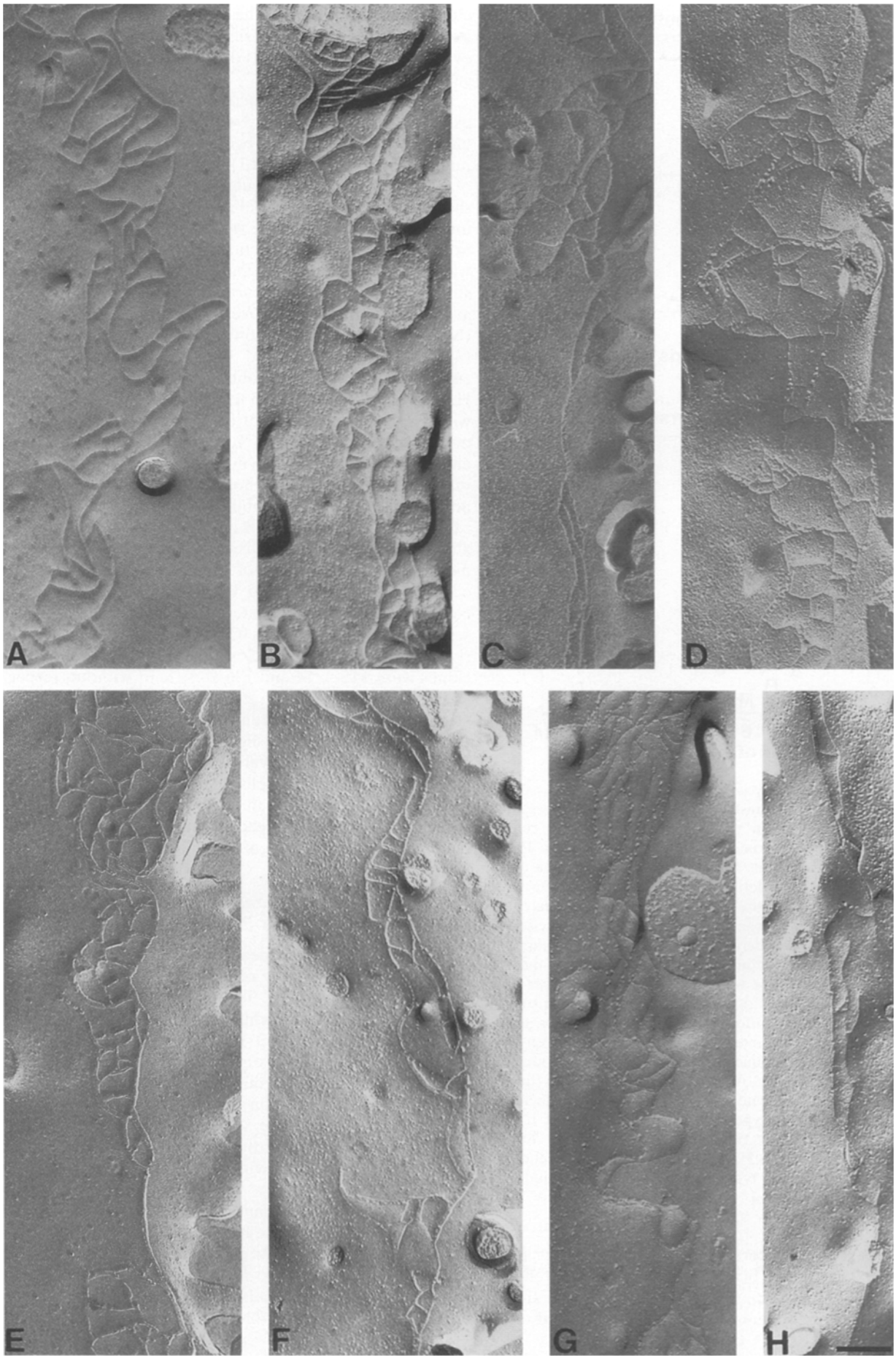
A
B
C
D
E
F
G
H

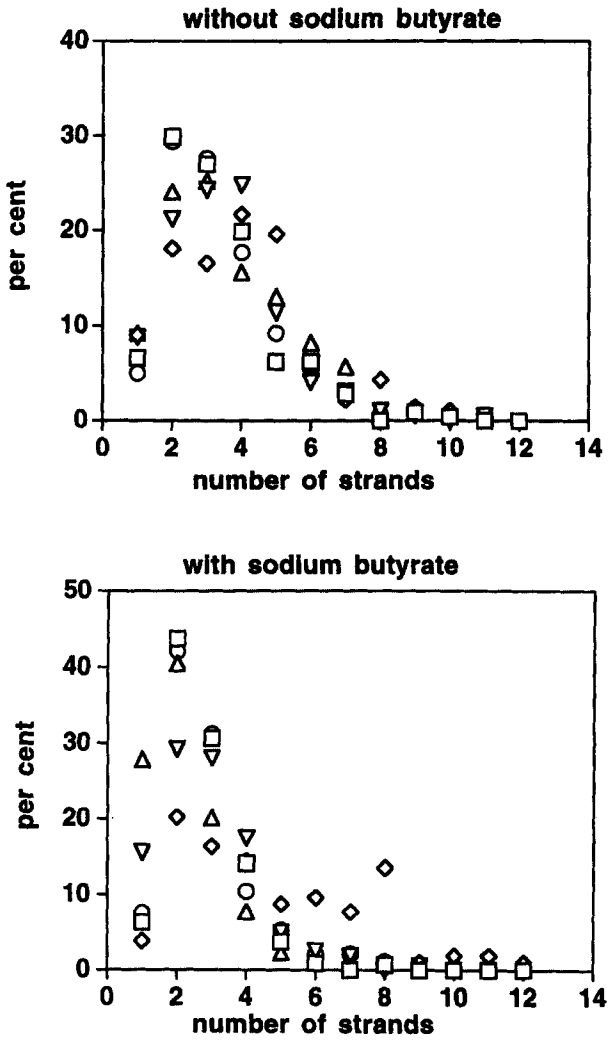

Figure 12. Quantitative analysis of freeze-fracture replicas derived from wild-type and transfected MDCK cells. Images of freeze-fractures derived from wild-type and transfected cells were quantified as described under Material and Methods. The values for control transfections and cells expressing chicken occludin or HAoccludin were derived from single clones, and the ones for HAoccludinCT3 were generated from two different clones. The number of junctional segments scored in each clone was between 104 and 278 (derived from 9–12 images), corresponding to 20–55 μm of tight junctions. The distribution of junctional strands in a given clone was computed by the number of times (n_i) it consisted of 1, 2, . . . , i strands. To ease comparisons between the distribution of different clones of MDCK cells, the total number of segments counted in a given clone was taken as 100% and segments of tight junctions having 1, 2, . . . , i strands were expressed as percentage. Average number of strands (first value, without sodium butyrate; second value, in parenthesis, with sodium butyrate): wild-type MDCK, 3.2 ± 1.6 (2.7 ± 1.1); occludin, 3.8 ± 1.9 (4.7 ± 2.6), HAoccludin 3.5 ± 1.7 (2.9 ± 1.4), HAoccludinCT3, 3.6 ± 1.9 (2.3 ± 1.4), and control transfection, 3.5 ± 1.9 (2.7 ± 1.2). □, wild type; ◇, occludin; ▽, HAoccludin; △, HAoccludinCT3; ○, control.

change occurred in cells expressing HAoccludin (3.5 ± 1.7 without and 2.9 ± 1.4 with butyrate). While this difference could be due to clonal variation, it could also mean that the NH_2-terminal epitope interferes with a function of occludin in the formation of the intramembrane fibrils. Since both clones exhibited very similar increases in TER, however, the number of strands did not correlate with electrical resistance.

Since the fluorescence microscopy indicated that in cells expressing HAoccludinCT3 neither the transfected mutant nor the endogenous occludin formed a continuous junctional ring (Figs. 6 and 7), the freeze-fracture analysis of these cells was of particular interest. Fig. 11, *G* and *H* shows that these samples did not reveal a redistribution or unusual arrangement of the strands suggesting that disruption of the continuous junctional ring formed by occludin was not paralleled by apparent discontinuities in the strands. This was also supported by a quantification of the average length of the recovered junctional segments derived from cells with a continuous distribution of occludin (3.0 ± 0.6 μm without and 3.8 ± 1.1 μm with butyrate) compared with the ones obtained from cells expressing HAoccludinCT3 (3.2 ± 0.3 μm without and 3.5 ± 0.8 μm with butyrate; the length of the observed patches by immunofluorescence was ~1 μm). Furthermore, the presence of continuous intramembrane strands in freeze-fracture and the normal morphology in thin sections do also not suggest a general instability of tight junctions in cells expressing HAoccludinCT3 that results in morphological alterations upon chemical fixation and thereby caused the discontinuous distribution of endogenous and transfected occludin that we observed by fluorescence microscopy. Nevertheless, butyrate-treated samples appeared to possess slightly fewer strands. Quantification of images derived from two different clones (TER values of the two clones were 145 ± 14 and 136 ± 8 Ωcm^2 without, respectively, 195 ± 23 and 145 ± 12 Ωcm^2 with butyrate) revealed no dramatic differences in the distribution of the strands but confirmed the slight reduction since, after treatment with butyrate, the average number of strands was reduced to 2.3 ± 1.4 in cells expressing HAoccludinCT3 compared with 2.7 ± 1.1 in wild-type cells. Thus, expression of HAoccludinCT3 leads to higher TER values without causing the formation of more junctional strands.

Expression of Wild-type and Mutant Occludin Results in Increased Paracellular Permeability

Tight junctions do not appear to be simple seals but rather to allow selective passage of certain components through the paracellular pathway. Therefore, the existence of selective channels within tight junctions had been proposed (Claude, 1978; Cereijido et al., 1989). It would be conceivable that occludin forms or participates in the formation of those hypothetical selective channels in tight junctions. To test whether expression of wild-type or mutant occludin has any effect on the selective permeability of tight junctions we measured diffusion of fluorescently labeled dextran (FITC-dextran) with an average molecular mass of 4 kD.

Fig. 13 *A* shows the amount of 4 kD FITC-dextran diffusion from the apical to the basolateral side of monolayers formed by wild-type and transfected cells over a period of 3 h at 37°C normalized to the value obtained from wild-type MDCK cells (top panel without and bottom panel with an overnight incubation with sodium butyrate). With-

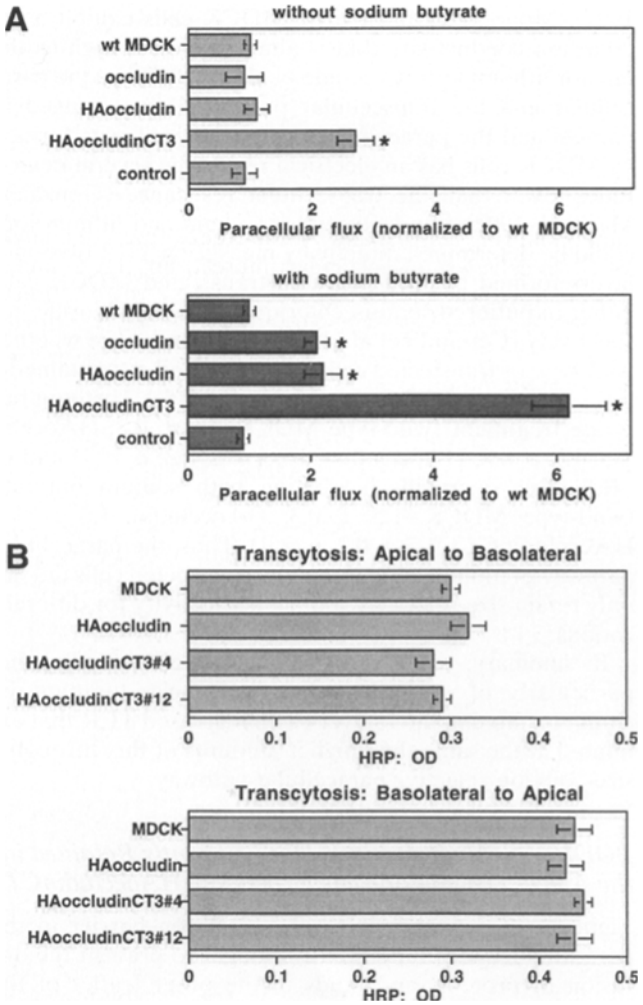

Figure. 13. Paracellular flux of monolayers formed by cells expressing wild-type and mutant chicken occludin. (*A*) Wild-type (*wt MDCK*) and transfected cell lines were cultured on filters and paracellular flux of 4 kD FITC-dextran was measured in the apical to basolateral direction without (*top panel*) or with (*bottom panel*) induction with sodium butyrate. The amount of FITC-dextran diffused to the basolateral side of the monolayer was normalized by the average value obtained from wild-type cells. Values given represent mean values (± 1 SD) of three independent determinations performed in duplicate using two independent clones of each transfection. The ratio of the mean value of flux measured in wild-type MDCK cells not treated with butyrate divided by the one obtained from butyrate treated wild-type cells was 1.1 ± 0.2. Bars labeled with an asterisk represent values that are significantly ($P < 0.001$ in a t test) bigger than the ones obtained from wild-type MDCK cells. (*B*) Fluid-phase transcytosis of butyrate-induced, wild-type and transfected MDCK cells was measured by allowing the cells to internalize HRP for 10 min from either the apical (*top panel*) or basolateral (*bottom panel*) side. After cooling and washing the cells on ice, the monolayers were brought back to 37°C for 90 min. Transcytosis was then assayed by determining HRP activity transported across the monolayers. Values represent the means (± 1 SD) of two independent determinations performed in duplicate. The results for two different clones of HAoccludinCT3-expressing cells are shown.

out butyrate induction, cells expressing either chicken occludin or HAoccludin did not reveal more transepithelial diffusion. If higher expression levels of the transfected proteins were induced by sodium butyrate, however, the values increased by a factor of 2 compared with wild-type cells or cells transfected with a control cDNA (LDL receptor). In contrast, monolayers formed by HAoccludinCT3-expressing cells revealed more transepithelial diffusion (by a factor of 3) without the butyrate treatment. Since these cells did not exhibit fewer strands in freeze-fracture than wild-type cells (Fig. 12), the number of strands also does not correlate with paracellular flux. If expression of HAoccludinCT3 was further enhanced by incubation with sodium butyrate, paracellular flux exhibited even higher increases.

Since our assay measures total transepithelial transport, these results could be due to either increased rates of transcytosis or enhanced paracellular flux. To differentiate between the two possibilities, we measured fluid-phase transcytosis by allowing butyrate-treated cells to take up HRP on either the apical or basolateral cell surface domain for 10 min at 37°C. The cells were then cooled on ice, washed to remove any noninternalized peroxidase, and brought back to 37°C for 90 min. Basolateral and apical media were collected and assayed for peroxidase activity. Fig. 13 *B* shows that cells expressing either HAoccludin or HAoccludinCT3 (the results of two different clones are shown) did not exhibit any difference in the amounts of transcellular fluid phase transport. Furthermore, transcytotic fluid phase transport in the basolateral to apical direction is ~50% higher than in the apical to basolateral direction (Fig. 13 *B*), while the absolute amount of FITC-dextran diffusion was found to be the same in both directions (not shown). Thus, increased rates of transcytosis cannot account for the up to six times higher amounts of transepithelial diffusion of 4 kD FITC-dextran in transfected cells indicating that this must be due to increased paracellular flux. Since all of these transfected cells established monolayers electrically at least twice as tight as those formed by wild-type MDCK cells (Figs. 5 and 10), the expression of wild-type chicken occludin and, particularly, of HAoccludinCT3 led to a functional dissociation of paracellular permeability and electrical resistance.

Paracellular Pathway in Transfected Cells Is Size and Ion Selective

Several experiments in the literature suggest that the paracellular pathway of epithelia behaves as an aqueous pathway that restricts solute permeation on the basis of size and charge (Cereijido, 1991). To test whether the amount of paracellular flux in transfected cells depends on the size of the analyzed tracer we measured paracellular diffusion of [^{3}H]mannitol (182 D), 40 kD FITC-dextran, HRP (44 kD), and 400 kD FITC-dextran across sodium butyrate–treated monolayers formed by wild-type and transfected cells.

Monolayers of cells expressing chicken occludin (Fig. 14) and HAoccludin (not shown) only exhibited clearly higher amounts of paracellular diffusion if tracers with a small molecular weight were used ([^{3}H]mannitol and 4 kD FITC-dextran). If HAoccludinCT3-transfected cells were analyzed, however, 40 kD dextran and HRP also diffused

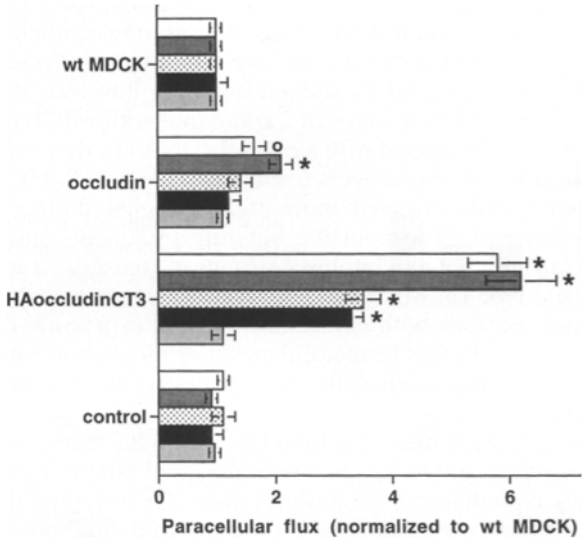

Figure 14. Paracellular flux in wild-type and transfected cells depends on the size of the tracer. Paracellular flux of various hydrophilic tracers in the apical to basolateral direction of butyrate-induced monolayers formed by wild-type or transfected cells, respectively, was measured as in Fig. 13 *A* (the values for 4 kD FITC-dextran are again given to facilitate comparison). The numbers for each tracer were normalized to the corresponding value obtained from wild-type cells. Shown are means (± 1 SD) of at least two independent experiments performed in duplicate. In the case of occludin and HAoccludinCT3, two independent clones were used. Labeled bars are significantly (*asterisk*, $P < 0.001$; *circle*, $P < 0.02$ in a t test) bigger than the ones obtained from wild-type MDCK cells. □, mannitol; ■, 4 kD Dextran; ▩, 40 kD dextran; ■, HRP; ▨, 400 kD dextran.

through the monolayers to a larger extent than in wild-type cells. Nevertheless, with 400 kD FITC-dextran we did not measure higher rates of diffusion in any analyzed cell line. Thus, the paracellular pathway in monolayers formed by cells expressing wild-type and mutant chicken occludin is still size selective.

If the size selectivity in transfected cells would be the same as in wild-type cells, one would not expect to see a significant difference in the relative increase in permeability between small and high molecular weight tracers. Our assay, however, measures total transepithelial transport (i.e., paracellular flux and transcellular fluid-phase transport) and the absolute values for transepithelial flux decrease for transfected and wild-type cells if the molecular weight of the tracer increases (not shown); hence, the contribution of fluid-phase transport by transcytosis is more significant for the high molecular weight tracers than it was found to be for 4 kD FITC-dextran. Consequently, one has to expect a lower increase of transepithelial transport of bigger tracers since only paracellular flux and not transcytosis was altered by the transfections. Therefore, our tracer studies suggest that the paracellular pathway in cultures of transfected cells discriminates not only between tracers of different sizes but appears to possess an at least superficially similar size-selectivity as the one in monolayers of wild-type MDCK cells.

Another measure for the selectivity of the paracellular pathway is its conductivity for different types of ions (Reuss, 1991). Monolayers formed by MDCK cells exhibit a sodium ion conductivity that is almost twice as high as the one for lithium ions (Cereijido et al., 1978). Since the paracellular and the transcellular pathways are arranged in parallel and the paracellular route of monolayers formed by MDCK cells has an electrical resistance several magnitudes lower than the transcellular resistance (González-Mariscal, 1991), conductivity for sodium and lithium ions could be determined directly by measuring TER of monolayers formed by wild-type and transfected MDCK cells either in buffered sodium chloride or lithium chloride, respectively (Cereijido et al., 1978). Independent of whether wild-type or transfected cells were analyzed, we obtained a ratio of sodium to lithium conductivity of ~1.7 without butyrate treatment (wild-type MDCK, 1.8 ± 0.3; HAoccludin, 1.7 ± 0.2; HAoccludinCT3, 1.7 ± 0.3; $n = 4$) and of ~1.5 after overnight incubation with sodium butyrate (wild-type MDCK, 1.5 ± 0.3; HAoccludin, 1.6 ± 0.3; HAoccludinCT3, 1.5 ± 0.2; $n = 4$). Thus, the paracellular pathway of monolayers formed by transfected cells did not only retain size-selectivity but also selectivity for different cations.

In summary, the expression of chicken occludin and, particularly, of a COOH-terminally truncated mutant occludin resulted in monolayers with increased TER that exhibited at the same time higher amounts of flux through a size- and ion-selective paracellular pathway.

BODIPY-Sphingomyelin Is Not Efficiently Retained in the Apical Domain of Cells Expressing HAoccludinCT3

Tight junctions not only form a diffusion barrier in the paracellular space but are also thought to prevent the diffusion of proteins and lipids in the outer leaflet of the plasma membrane between the apical and basolateral cell surface domains (Dragsten et al., 1981; van Meer and Simons, 1986). To test whether transfection of wild-type or mutant chicken occludin affected this second function of tight junctions we labeled the apical cell surface of butyrate-treated monolayers grown on filters with BODIPY-sphingomyelin for 10 min at 4°C. The cells were then washed and left for an additional 60 min on ice before observation by confocal microscopy. A similar assay has recently been used to test for the presence of an intact intramembrane diffusion barrier in ATP-depleted MDCK cells (Mandel et al., 1993).

The z-sections shown in Fig. 15 *A* demonstrate that wild-type and HAoccludin-transfected MDCK cells retained the fluorescent lipid in the apical plasma membrane. In cells expressing HAoccludinCT3, however, the fluorescent lipid started to diffuse through the tight junctions and labeled the lateral plasma membrane. If the cells were analyzed immediately after the labeling phase, only the apical membrane was stained; therefore, the lateral staining after 60 min could not be due to the increased amounts of paracellular flux (Fig. 15 *A*: 0 min). Additionally, at the temperature the cells were labeled, on ice for 10 min, paracellular diffusion of 4 kD FITC-dextran over a period of 3 h was very low and no diffusion of 40 kD FITC-dextran (still smaller than BSA) could be detected (not shown). Since it could be that the junctions of cells expressing the mutant occludin are more sensitive to the manipulations required

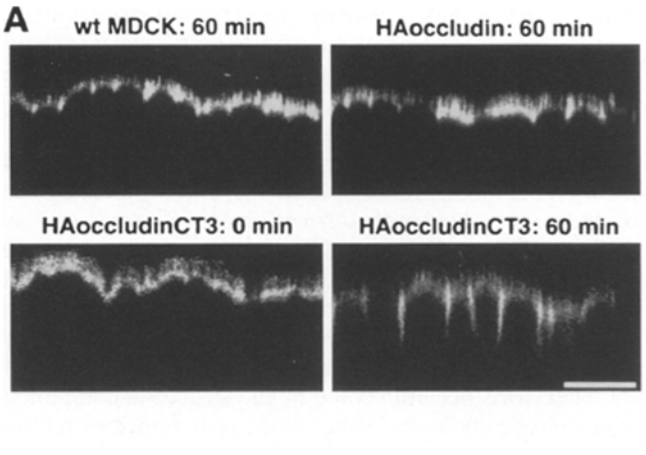

Figure 15. Lateral diffusion of BODIPY-sphingomyelin in wild-type and transfected MDCK cells. (*A*) The apical surface of filter-grown and butyrate-treated cells was labeled for 10 min with BODIPY-sphingomyelin/BSA complexes on ice. Then, the cells were immediately mounted (0 min) or left for an additional 60 min on ice. The distribution of the fluorescent lipid was then analyzed by z-sectioning. Bar, 10 μm. (*B*) The apical surface of filter-grown and butyrate-treated cells was labeled on ice as in *A*. The cells were then washed and cold buffer containing defatted BSA was added to the basolateral side to back exchange fluorescent lipid diffused across tight junctions. After 1.5 h on ice, the BSA solutions were collected and the cells were lysed in Triton X-100. The fluorescence in both extracts was measured and the amount of diffusion was normalized by the total recovered fluorescence. If cells were not treated with butyrate, a two to threefold difference was observed between wild-type MDCK and HAoccludinCT3-expressing cells (not shown). Values are means (± 1 SD) of two independent experiments performed in triplicate (two independent clones per transfection).

for microscopical observation, we tested whether the fluorescent lipid would also diffuse across tight junctions if the cells were left at 4°C. To do this, cells were labeled with BODIPY-sphingomyelin and washed. Defatted bovine serum albumin was then added to the basolateral side for 1.5 h on ice to back exchange fluorescent lipid diffused to the basolateral plasma membrane. Basolaterally extracted fluorescence and Triton X-100 extractable fluorescence still associated with cells at the end of the experiment were then determined with a fluorometer. Fig. 15 *B* shows that approximately five times more BODIPY-sphingomyelin diffused from the apical to the basolateral plasma membrane in cells expressing HAoccludinCT3 than in the other tested cell lines. Similar results were obtained if the cells were labeled basolaterally and extracted apically (not shown). These data demonstrate that cells expressing HAoccludinCT3 have a reduced capability to maintain BODIPY-sphingomyelin in a specific cell surface domain. Since the transfected mutant and the endogenous occludin were discontinuously distributed in these cells, this suggests that a continuous junctional ring of occludin is important to restrict diffusion of lipids in the outer leaflet of the plasma membrane and that occludin is involved in the formation of the intramembrane diffusion barrier between the apical and the basolateral cell surface domains.

We also tested whether expression of HAoccludinCT3 interferes with protein polarity. Using cell surface biotinylation, we did not find a significant difference in the cell surface distribution of Na^+/K^+-ATPase, a classical basolateral marker, and of total apically or basolaterally biotinylatable and Triton X-100-extractable proteins (not shown). Additionally, coexpression of an apically expressed mutant Fc receptor (Matter et al., 1992) did also not indicate a significant loss in protein polarity (not shown). While it is not possible yet to completely exclude any effect on polarity of specific proteins, it appears that lipid polarity is more sensitive to manipulations affecting the apical–basolateral intramembrane diffusion barrier.

Discussion

Our results demonstrate that expression of wild-type and, particularly, mutant occludin led to a functional dissociation of paracellular permeability and electrical resistance and show that this protein is also involved in the formation of the apical–basolateral intramembrane lipid diffusion barrier.

Assembly of Tight Junctions

In stably transfected MDCK cells, chicken occludin was efficiently sorted to tight junctions as previously published for transient expression experiments using bovine and human epithelial cells (Furuse et al., 1994). This suggests that occludin targeting and integration into tight junctions is a well-conserved process. The COOH-terminal cytoplasmic domain of occludin was found to be not required for targeting of transfected occludin since HAoccludinCT3 was expressed in tight junctions.

Deletions within the COOH-terminal domain of occludin were previously found to abolish transport to tight junctions in transiently transfected bovine kidney cells (Furuse et al., 1994). While it is not yet clear what caused this discrepancy, it might be due to the different types of constructs used in the two studies. While we were expressing a mutant occludin that lacked almost the entire COOH-terminal domain, Furuse et al. expressed constructs bearing only partial deletions of this domain and, furthermore, a COOH-terminal myc-epitope; hence the inhibition of targeting in the latter experiments could have been due to, for instance, folding problems caused by the residual parts of the COOH-terminal domain.

Expression of HAoccludinCT3 also resulted in a redistribution of endogenous occludin suggesting that endogenous and transfected occludin are interacting with each other in a direct or indirect manner. Therefore, mutant occludin could be transported to tight junctions due to this interaction and the fraction of HAoccludinCT3 that local-

izes to a perinuclear compartment might reflect protein that has not oligomerized with endogenous occludin. Therefore, how efficiently a COOH-terminally truncated mutant of occludin is transported to tight junctions might depend on the level of endogenous occludin. Thus, the above described discrepancy could also be due to different levels of endogenous occludin in the used cell lines. As a consequence, it is not possible to rule out that the COOH-terminal domain of occludin has a function in targeting. Since tight junctions are a subdomain of the basolateral membrane and cytoplasmic domain determinants have been shown to be required for basolateral transport of several membrane proteins (Matter and Mellman, 1994), it could be that the COOH-terminal cytosolic domain of occludin specifies transport to the basolateral cell surface. If linked to an apically expressed protein, this domain is indeed able to mediate basolateral transport, but not integration into tight junctions, of the chimeric membrane protein (Balda, M.S., and K. Matter, manuscript in preparation). After arriving at the basolateral plasma membrane, integration of occludin oligomers into tight junctions could then occur due to other interactions involving the NH_2-terminal half of the protein.

While deletion of the COOH-terminal domain of occludin did not abolish targeting of transfected chicken occludin, it did affect the distribution of the protein within tight junctions since it resulted in a discontinuous junctional staining pattern. Since this was observed under various fixation conditions, it is unlikely that the discontinuous distribution of HAoccludinCT3 was caused by fixation of a normally mobile membrane protein. Furthermore, since the same discontinuities in the distribution of HAoccludinCT3 were observed in cells fixed with paraformaldehyde and permeabilized with saponin, conditions that did not reveal any difference in the junctional morphology between cells expressing HAoccludin or HAoccludinCT3 by EM, the discontinuities were not caused by a vesiculation of the junction due to fixation and permeabilization. Therefore, the COOH-terminus appears to be required for the normal distribution of occludin within the junction. It is tempting to speculate that this is due to its capability to interact with ZO-1, a component of the submembrane cytoskeleton of tight junctions (Furuse et al., 1994). In HAoccludinCT3-expressing cells, ZO-1 exhibited only a gentle redistribution and was still forming a continuous junctional ring suggesting that its localization is at least not only determined by occludin but also by other junctional components or, more importantly, the cytoskeleton. Therefore, one could imagine that the continuous junctional belt of occludin is due to polymerized oligomers, containing occludin and perhaps other membrane proteins, that are lined up with the submembrane cytoskeleton due to an interaction between the COOH-terminal domain of occludin and ZO-1. In the absence of a sufficient number of such anchors, as in cells expressing HAoccludinCT3, the continuous belt collapses into patches due to a disturbed equilibrium between the two forces.

Intramembrane Diffusion Barrier and Cell Surface Polarity

Tight junctions are also thought to be important for the maintenance of biochemically distinct cell surface domains by forming an intramembrane fence that restricts the diffusion of lipids in the outer leaflet of the plasma membrane (Dragsten et al., 1981; van Meer and Simons, 1986). We show here that cells expressing HAoccludinCT3 were no longer capable of preventing diffusion of a fluorescent lipid from one cell surface domain to the other indicating that occludin is involved in the formation of the intramembrane diffusion fence. We were only able to detect significant amounts of lipid diffusion in cells expressing the discontinuously distributed, COOH-terminally truncated occludin suggesting that a continuous junctional belt of occludin is important for the maintenance of cell surface lipid polarity. Therefore, occludin could be the structural component which physically forms, either alone or together with other components, the intramembrane diffusion fence.

HAoccludinCT3-expressing cells, found to have lost the capability to maintain a fluorescent lipid in a specific cell surface domain, exhibited a higher TER than nontransfected wild-type cells. Thus, the structural properties of tight junctions responsible for the intramembrane fence and the electrical seal appear to be different. This is also supported by the effect of a short period of ATP depletion that resulted in a loss of TER but not in disruption of the intramembrane diffusion fence (Mandel et al., 1993). Furthermore, disruption of the intramembrane fence after longer periods of time of ATP depletion correlated with fragmentation of the intramembrane strands of tight junctions and disruption of the continuous junctional ring formed by ZO-1 (Bacallao et al., 1994). While we observed a slightly changing distribution of ZO-1, we did not observe a fragmentation of the intramembrane strands. Nevertheless, we observed a slight reduction in the average number of strands in butyrate-treated, HAoccludinCT3-expressing cells, suggesting that an efficiently working intramembrane diffusion fence may require several intramembrane strands. Alternatively, redistribution of occludin may have affected the structural and functional properties of the intramembrane strands (see below).

Expression of HAoccludinCT3 did not significantly affect polarity of Na^+K^+-ATPase and of Triton X-100–extractable proteins. While Na^+K^+-ATPase might be retained in the basolateral plasma membrane due to its interaction with the actin-based cytoskeleton (Nelson and Veshnock, 1987), Triton X-100–extractable proteins should be more mobile and, therefore, one would have expected to detect an altered cell surface distribution in cells expressing HAoccludinCT3. It is difficult to rule out that this difference between proteins and lipids is not due to an incomplete disruption of the intramembrane diffusion barrier. Our data indicate, however, that lipid polarity is at least more sensitive to manipulations affecting the intramembrane fence. On one hand, this might be due to interactions between membrane proteins and the cytoskeleton that restrict lateral mobility (Vega-Salas et al., 1987; Nelson, 1992) and, on the other hand, many mobile membrane proteins possess bulky extracellular domains suggesting that the paracellular barrier must be as important for protein polarity as the intramembrane diffusion fence.

Paracellular Permeability and Electrical Resistance

Expression of full-length and COOH-terminally truncated

chicken occludin resulted in a significant increase in TER. In MDCK cells, the transcellular pathway has an electrical resistance about two orders of magnitude higher than the paracellular pathway (González-Mariscal et al., 1989). Since these two pathways can be thought of as two resistors arranged in parallel, the measured increase in TER reflects an increase in the resistance of the paracellular pathway. Furthermore, this increase was dependent on the amount of expressed protein since induction of higher expression levels led to a further stimulation of TER. Since chicken occludin was properly targeted, this suggests that occludin is involved in the formation of sealed tight junctions. Similar results were obtained independently with a different expression system in which expression of occludin in MDCK cells was induced with isopropyl thiogalactoside and resulted in a 40% increase of TER (McCarthy, et al., 1996).

Fluorescence microscopy of cells expressing HAoccludin CT3 indicated that the transfected mutant and endogenous occludin did not form a continuous junctional belt but colocalized in patches along the junction. Since this was observed after various different fixation techniques and these monolayers still exhibited increased TER, a continuous junctional distribution of occludin does not appear to be required for the formation of electrically tight epithelial monolayers. Since the parts of tight junctions that did not contain occludin in HAoccludinCT3-expressing cells represented a considerable fraction of the total tight junction, these parts are rather unlikely to have lost most of their electrical resistance. It is not clear whether this means that occludin is not at all a structural component of the paracellular diffusion barrier or whether its gaps are filled with one or more unknown structural components of tight junctions that are not stably associated with occludin. The increase in TER in transfected cells, however, could also be due to a function of occludin in the assembly or stabilization of the paracellular diffusion barrier.

Expression of full-length, and particularly, COOH-terminally truncated occludin resulted in electrically tighter junctions and increased paracellular permeability but did not significantly affect the size and ion selectivity of the paracellular pathway. This and the fact that MDCK cells express occludin endogenously indicate that expression of exogenous occludin induced higher levels of activity of an existing mechanism that allows selective diffusion through electrically sealed tight junctions. Since monolayers of cells expressing HAoccludinCT3 exhibited much more paracellular flux than cultures of cells expressing comparable amounts of full-length chicken occludin or HAoccludin, the COOH-terminal cytosolic domain might be important for the regulation of the paracellular pathway. It is not clear yet, however, whether increased paracellular flux in cells expressing HAoccludinCT3 is a consequence of the clustering of occludin or whether paracellular flux and occludin distribution within the junction are not directly related to each other but are both controlled by the COOH-terminal cytoplasmic domain.

The functional dissociation of paracellular permeability from electrical resistance was rather surprising since the two parameters had generally been considered to measure the same characteristics of tight junctions. Nevertheless, TER is an instantaneous measurement, and paracellular flux measures permeability during a longer period of time; hence TER is an instantaneous measurement that reflects the permeability at a given point in time, and paracellular flux is an indicator for the permeability over a period of time. One possibility to explain how these two parameters can change in opposite directions is the model proposed by Claude and modified by Cereijido et al. (Claude, 1978; Cereijido et al., 1989). According to this hypothesis, tight junctions are a series of one or more diffusion barriers. Each of these diffusion barriers, however, is not always tightly sealed but open and closes in a fluctuating fashion. Thus, electrical resistance is a measure of the number of closed barriers at a given point in time. Since the paracellular pathway is size and ion selective, this opening and closing was attributed to aqueous channels within each diffusion barrier. That permeation of junctions by relatively large molecules and ions involves the same aqueous pores was suggested by several observations. Since the ion selectivity of the paracellular pathway is much lower than the selectivity of cell membranes, junctional permeation of ions must include relatively large channels. This is also supported by the linear current–voltage relationship over a large current range (for review see Reuss, 1991). Since the ion selectivity of the paracellular pathway was changed by acidification or the addition of polyvalent cations, it was proposed that its size and ion selectivity are a result of relatively large pores containing dipoles with negative sides oriented toward the aqueous phase (Wright and Diamond, 1968; Moreno and Diamond, 1975; Cereijido et al., 1978; Reuss, 1991).

Compartmentalization of these channels (for instance, by a similar network as the one formed by the intramembrane strands) is not only required for a model with several barriers to work, but also explains why such fluctuating channels do not lead to fluctuating TER values (Cereijido et al., 1989). There would be thousands of such compartments in a given monolayer; hence there would be no big fluctuations in the number of open compartments at any given time. If flux of a tracer is measured, however, it starts to enter into the junctions if the first diffusion barrier is open and can go on at a later point in time when the next layer opens and the first layer is already closed again. As a consequence, a tracer could migrate layer by layer through tight junctions which as a unit were electrically sealed during the entire process.

We found here that expression of full-length and particularly COOH-terminally truncated occludin in MDCK cells caused increased paracellular flux without having any apparent effect on the selectivity of the paracellular pathway. Therefore, occludin could be involved in the formation or regulation of these fluctuating aqueous channels and, therefore, cause the increased paracellular flux in transfected cells. Since transfected HAoccludinCT3 changed the distribution of endogenous occludin and the distribution of occludin in one cell influenced the distribution of occludin in neighboring cells, it could be that occludin molecules and, perhaps, other membrane components of neighboring cells come together and form a channel that allows selective paracellular permeability. Since the COOH-terminal cytoplasmic domain has been shown to interact with ZO-1 in vitro (Furuse et al., 1994) and its deletion caused a stronger increase in paracellular flux, the

channel forming or activating function of occludin might be regulated by the submembrane cytoskeleton. A model in which interactions between the submembrane cytoskeleton and the COOH-terminal cytoplasmic domain of occludin regulate paracellular permeability could also explain an apparent discrepancy between our results and the ones by McCarthy et al. where the presence of isopropyl thiogalactoside, which induces occludin expression in their experimental system, had a negative effect on paracellular flux (McCarthy, et al., 1996). In our experiments, expression of full-length occludin resulted either in no change in paracellular flux or, at high expression levels induced by sodium butyrate, in a slight increase. This together with the relatively moderate increase in TER in the experiments by McCarthy et al. (the increase in TER was ~40% compared with at least twice as much in all of our clones) could mean that there are sufficient free binding sites (e.g., ZO-1 molecules) to interact with transfected occludin at low levels of expression; hence only the sealing capacity, which increases TER, of occludin is observed. With increasing expression levels, however, those binding sites would become saturated and a fraction of the transfected occludin would no longer be capable to interact with the submembrane cytoskeleton resulting in an activation of the channel forming or regulating capabilities of occludin.

In freeze-fracture replicas, tight junctions can be seen as a set of interconnected fibrils composed of intramembrane particles (Staehelin, 1973). One could imagine that each of this fibrils represents a diffusion barrier. Since they are arranged as a network and not in a parallel array, they would also provide the above mentioned required compartmentalization of the paracellular pathway (Cereijido et al., 1989). Furthermore, there is an exponential relationship between the number of strands and the TER of an epithelial tissue further suggesting that these strands could be the diffusion barrier and contain fluctuating channels (Claude, 1978). Nevertheless, there is no direct evidence for the strands being the diffusion barriers and their number does not always correlate with TER (Martínez-Palomo and Erlij, 1975; Stevenson et al., 1988; González-Mariscal et al., 1989). Similarly, expression of HAoccludinCT3 led to higher TER values and rather less than more intramembrane strands. Furthermore, Mandel et al. demonstrated that short times of ATP depletion essentially eliminated TER without affecting the number of intramembrane strands (Mandel et al., 1993). Therefore, these authors suggested that the paracellular diffusion barrier is not due to the sheer presence of the strands but to an interaction of two strands from neighboring cells. Since our experiments suggest that occludin is part of a complex that forms cell–cell contacts, it could be that occludin is involved in this interaction between neighboring strands and, therefore, its overexpression increases TER. This idea is supported by the finding that occludin localizes to the intramembrane strands in freeze fractures (Furuse et al., 1996). Nevertheless, this observation does not necessarily mean that the paracellular diffusion barriers are due to interacting pairs of strands but could also signify that different properties of the same junctional components (one of them being occludin) are involved in the formation of the intramembrane strands (i.e., transmembrane domains) and in the paracellular diffusion barrier (i.e., extracellular domains). Interestingly, if occludin was overexpressed in insect cells, multilamellar structures were induced that appeared to consist of pairs of closely associated membrane bilayers suggesting that occludin may have an adhesive property (Furuse et al., 1996). Since a continuous junctional ring of occludin is apparently not required for an electrically tight monolayer, however, one would have to assume that there are other junctional components that also strengthen this interaction and fill the parts left empty by occludin in cells expressing HAoccludinCT3.

The same is true for the intramembrane strands themselves. Since the discontinuous distribution of occludin was not paralleled by apparent interruptions of the strands in chemically fixed cells expressing HAoccludinCT3, occludin is quite unlikely be the only component of the intramembrane strands. At high expression levels induced by sodium butyrate, however, HAoccludinCT3-expressing cells had slightly fewer strands. In contrast, expression of wild-type chicken occludin induced a slight increase in the number of strands in our experiments as well as in those by McCarthy et al. (1996) suggesting that this protein might play a role in the generation or organization of the intramembrane strands. Interestingly, Furuse et al. reported that baculovirus-mediated overexpression of occludin in insect cells did not only induce the formation of multilamellar structures containing intramembrane particles but occasionally observed also very short strands (Furuse et al., 1996). This suggests that occludin might have the capabilities to contribute to the intramembrane strands of tight junctions but does not appear to be capable to form a complex network of strands by itself, even if it reaches very high local concentrations as in those multilamellar structures upon virus-mediated overexpression. Therefore, and because of the much lower expression levels of stably transfected cDNAs in mammalian cell lines than in the baculovirus system, it is not surprising that we did not observe dramatic changes in the patterns formed by the intramembrane strands in the freeze-fracture analysis.

The combination of the above-discussed channel hypothesis with the idea of occludin as a regulated channel-forming or -activating protein that is also involved in the interaction of neighboring plasma membranes and thereby helps to establish a series of paracellular diffusion barriers could explain several contradictory observations. First, TER does not always correlate with the number of strands (Martínez-Palomo and Erlij, 1975; Stevenson et al., 1988; González-Mariscal et al., 1989): TER would not directly depend on the number of strands but on how well neighboring plasma membranes are interconnected as well as on the open probability of the channels. Second, paracellular permeability does not always correlate with TER: TER does not and paracellular permeability does depend on the number of channels if they are either all open or all closed within one barrier of one compartment. Thus, TER depends on how well neighboring strands are interconnected and on the open probability of the channels while paracellular diffusion depends in addition on the number of open channels per barrier and compartment. Furthermore, extending the model by assuming that occludin (or rather its transmembrane domains) is just one of the components that form the intramembrane strands would explain another apparent contradiction. Cells expressing

HAoccludinCT3 lost the capability to maintain a lipid in a specific domain but did not exhibit discontinuous intramembrane strands. In contrast, Bacallao et al. reported a correlation between disruption of the strands and loss of the intramembrane diffusion fence after longer times of ATP depletion (Bacallao et al., 1994). Therefore, pieces of strands that lack occludin might have different functional properties.

Although occludin appears to play a key role in tight junctions, different properties of it appear to be important for different functions. Additionally, our data are difficult to reconcile with a single structural membrane component of tight junctions suggesting that we need to improve our understanding of the molecular composition of this important epithelial structure before we are able to explain more precisely how tight junctions form on one hand a diffusion barrier and on the other hand allow selective permeability.

We thank Drs. K.M. McCarthy, I.B. Skare, M.C. Stankewich, M. Furuse, S. Tsukita, R.A. Rogers, R.D. Lynch, and E.E. Schneeberger for sharing information before publication. We are grateful to Drs. Peter van der Sluijs, Ira Mellman, James M. Anderson, Hans-Peter Hauri, Michael Caplan, and Lukas Huber for providing antibodies and to Hector Vargas for valuable technical help.

J.A. Whitney is a fellow of the International Postdoctoral Fellows Program of the U.S. National Science Foundation (INT-9424028) and K. Matter is a fellow of the START program of the Swiss National Science Foundation (31-38794.93). This research was supported by the Swiss National Science Foundation (31-40420.94) and the Canton de Genève.

Received for publication 29 November 1995 and in revised form 14 May 1996.

References

Anderson, J.M., M.S. Balda, and A. Faming. 1993. The structure and regulation of tight junctions. *Curr. Opin. Cell Biol.* 5:772–778.

Anderson, J.M., B.R. Stevenson, L.A. Jesaitis, D.A. Goodenough, and M.S. Mooseker. 1988. Characterization of ZO-1, a protein component of the tight junction from mouse liver and Madin-Darby canine kidney cells. *J. Cell Biol.* 106:1141–1149.

Bacallao, R., A. Garfinkel, S. Monke, G. Zamighi, and L.J. Mandel. 1994. ATP depletion: a novel method to study junctional properties in epithelial tissues. I. Rearrangement of the actin cytoskeleton. *J. Cell Sci.* 107:3301–3313.

Balda, M.S., L. González-Mariscal, K. Matter, M. Cereijido, and J.M. Anderson. 1993. Assembly of tight junctions: the role of diacylglycerol. *J. Cell Biol.* 123:293–302.

Cereijido, M. 1991. Evolution of ideas on the tight junction. *In* Tight Junctions. M. Cereijido, editor. CRC Press, Inc., Boca Raton, FL. 1–13.

Cereijido, M., L. González-Mariscal, and G. Contreras. 1989. Tight junction: barrier between higher organisms and environment. *News Physiol. Sci.* 4:72–74.

Cereijido, M., E.S. Robbins, W.J. Dolan, C.A. Rotunno, and D.D. Sabatini. 1978. Polarized monolayers formed by epithelial cells on a permeable and translucent support. *J. Cell Biol.* 77:853–880.

Cereijido, M., O. Ruiz, L. González-Mariscal, R.G. Contreras, M.S. Balda, and M.R. Garcia-Villegas. 1993. The paracellular pathway: a small version of the kidney nephron. *In* Biological Barriers to Protein Delivery. K.L. Audus and T.J. Raub, editors. Plenum Press, New York. 3–21.

Claude, P. 1978. Morphological factors influencing transepithelial permeability: a model for the resistance of the zonula occludens. *J. Membr. Biol.* 39:219–232.

Daro, E., P. van der Sluijs, T. Galli, and I. Mellman. 1996. Rab4 and cellubrevin define different early endosome populations on the pathway of transferrin receptor recycling. *Proc. Natl. Acad. Sci. USA.* In press.

Dragsten, P.R., R. Blumenthal, and J.S. Handler. 1981. Membrane asymmetry in epithelia: is the tight junction a barrier to diffusion in the plasma membrane? *Nature (Lond.).* 294:718–722.

Fallon, M.B., A.R. Brecher, M.S. Balda, K. Matter, and J.M. Anderson. 1995. Altered hepatic localization and expression of occludin after common bile duct ligation. *Am. J. Physiol.* 269:C1057–C1062.

Farquhar, M.G., and G.E. Palade. 1963. Junctional complexes in various epithelia. *J. Cell Biol.* 17:375–412.

Furuse, M., K. Fujimoto, N. Sato, T. Hirase, S. Tsukita, and S. Tsukita. 1996. Overexpression of occludin, a tight junction integral membrane protein, induces the formation of intracellular multilamellar bodies bearing tight junction-like structures. *J. Cell Sci.* 109:429–435.

Furuse, M., T. Hirase, M. Itoh, A. Nagafuchi, S. Yonemura, S. Tsukita, and S. Tsukita. 1993. Occludin: a novel integral membrane protein localizing at tight junctions. *J. Cell Biol.* 123:1777–1788.

Furuse, M., M. Itoh, T. Hirase, A. Nagafuchi, S. Yonemura, S. Tsukita, and S. Tsukita. 1994. Direct association of occludin with ZO-1 and its possible involvement in the localization of occludin at tight junctions. *J. Cell Biol.* 127: 1617–1626.

González-Mariscal, L. 1991. The relationship between structure and function of tight junctions. *In* Tight Junctions. M. Cereijido, editor. CRC Press, Inc., Boca Raton, FL. 67–76.

González-Mariscal, L., B. Chávez de Ramirez, A. Lázaro, and M. Cereijido. 1989. Establishment of tight junctions between cells from different animal species and different sealing capacities. *J. Membr. Biol.* 107:43–56.

Huber, L.A., S. Pimplikar, R.G. Parton, H. Virta, M. Zerial, and K. Simons. 1993. Rab8, a small GTPase involved in vesicular traffic between the TGN and the basolateral membrane. *J. Cell Biol.* 123:35–45.

Hunziker, W., J.A. Whitney, and I. Mellman. 1991. Selective inhibition of transcytosis in MDCK cells by brefeldin A. *Cell.* 67:617–627.

Kozak, M. 1989. The scanning model for translation: an update. *J. Cell Biol.* 108:229–241.

Lindemann, B., and A.K. Solomon. 1962. Permeability of luminal surface of intestinal mucosal cells. *J. Gen. Physiol.* 45:801–810.

Mandel, L.J., R. Bacallao, and G. Zampighi. 1993. Uncoupling of the molecular fence and paracellular gate function in epithelial tight junctions. *Nature (Lond.).* 361:552–555.

Martínez-Palomo, A., and D. Erlij. 1975. Structure of tight junctions in epithelia with different permeability. *Proc. Natl. Acad. Sci. USA.* 72:4487–4491.

Matter, K., W. Hunziker, and I. Mellman. 1992. Basolateral sorting of LDL receptor in MDCK cells: the cytoplasmic domain contains two tyrosine-dependent targeting determinants. *Cell.* 71:741–753.

Matter, K., and I. Mellman. 1994. Mechanisms of cell polarity: sorting and transport in epithelial cells. *Curr. Opin. Cell Biol.* 6:545–554.

Matter, K., J.A. Whitney, E.M. Yamamoto, and I. Mellman. 1993. Common signals control LDL receptor sorting in endosomes and the Golgi complex of MDCK cells. *Cell.* 74:1053–1064.

Matter, K., E.M. Yamamoto, and I. Mellman. 1994. Structural requirements and sequence motifs for polarized sorting and endocytosis of LDL and Fc receptors in MDCK cells. *J. Cell Biol.* 126:991–1004.

McCarthy, K.M., I.B. Skare, M.C. Stankewich, M. Furuse, S. Tsukita, R.A. Rogers, R.D. Lynch, and E.E. Schneeberger. 1996. Occludin is a functional component of the tight junction. *J. Cell. Sci.* In press.

Moreno, J.H., and J.M. Diamond. 1975. Cation permeation mechansims and cation selectivity in "tight junctions" of gallbladder epithelium. *In* Membranes. A Series of Advances. Vol. 3. Lipid Bilayers and Biological Membranes: Dynamic Properties. G. Eisenman, editor. Marcel Dekker, Inc., New York. 383–497.

Nelson, W.J. 1992. Regulation of cell surface polarity from bacteria to mammals. *Science (Wash. DC).* 258:948–954.

Nelson, W.J., and P.J. Veshnock. 1987. Ankyrin binding to (Na^+-K^+)ATPase and implications for the organization of membrane domains in polarized cells. *Nature (Lond.).* 328:533–536.

Pagano, R.E., and O.C. Martin. 1994. Use of fluorescent analogs of ceramide to study the Golgi apparatus of animal cells. *In* Cell Biology: A Laboratory Handbook. J.E. Celis, editor. Academic Press, Inc., San Diego, CA. 387–393.

Reuss, L. 1991. Tight junction permeability to ions and water. *In* Tight Junctions. M. Cereijido, editor. CRC Press, Inc., Boca Raton, FL. 49–65.

Staehelin, L.A. 1973. Further observations of the fine structure of freeze-cleaved tight junctions. *J. Cell Sci.* 13:763–786.

Stevenson, B.R., J.M. Anderson, D.A. Goodenough, and M.S. Mooseker. 1988. Tight junction structure and ZO-1 content are identical in two strains of Madin-Darby canine kidney cells which differ in transepithelial resistance. *J. Cell Biol.* 107:2401–2408.

Stevenson, B.R., M.B. Heintzelman, J.M. Anderson, S. Citi, and M.S. Mooseker. 1989. ZO-1 and cingulin: tight junction proteins with distinct identities and localizations. *Am. J. Physiol.* 257:C621–C628.

van Meer, G., and K. Simons. 1986. The function of tight junctions in maintaining differences in lipid composition between the apical and the basolateral cell surface domains of MDCK cells. *EMBO (Eur. Mol. Biol. Organ.) J.* 5: 1455–1464.

van Os, C.H., M.D. de Jong, and J.F.G. Slegers. 1974. Dimensions of polar pathways through rabbit gallbladder epithelium. *J. Membr. Biol.* 15:363–382.

Vega-Salas, D.E., P.J.I. Salas, D. Gundersen, and E. Rodriguez-Boulan. 1987. Formation of the apical pole of epithelial (Madin-Darby canine kidney) cells: polarity of an apical protein is independent of tight junctions while segregation of a basolateral marker requires cell-cell interactions. *J. Cell Biol.* 104:905–916.

Wright, E.M., and J.M. Diamond. 1968. Effects of pH and and polyvalent cations on the selective permeability of gallbladder epithelium to monovalent ions. *Biochim. Biophys. Acta.* 163:57–74.